Electronic Supplementary Material (ESI) for Journal of Materials Chemistry A.

Electronic Supplementary Information

Dynamic weak coordination bonding of chlorocarbons enhances the catalytic performance of a metal-organic framework material

Sun Ho Park,[a] Ricardo A. Peralta,*[a,b] Dohyun Moon,[c] and Nak Cheon Jeong*[a,b]

[a]Department of Physics and Chemistry, DGIST, Daegu 42988, Korea
E-mail: nc@dgist.ac.kr
[b]Center for Basic Science, DGIST, Daegu 42988, Korea
[c]Beamline Department, Pohang Accelerator Laboratory, Pohang 37673, Korea
E-mail: dmoon@postech.ac.kr

Table of contents

Section S1. Materials and Methods

Materials. All reagents were obtained from commercial sources (Sigma Aldrich, Alfa Aesar, or Daejung). Copper(II) nitrate hemipentahydrate ($Cu(NO_3)_2 \cdot 2.5H_2O$, 98%, Aldrich), trimesic acid (1,3,5-benzene tricarboxylic acid, H_3BTC, 98%, alfa), ethanol (EtOH, 94.5%, Daejung), N,N-dimethylformamide (DMF, 99.5% Daejung), and distilled deionized water (DDW) were used for the synthesis of small crystals of HKUST-1. Copper (II) chloride dihydrate ($CuCl_2 \cdot 2H_2O$, 99%, Aldrich) and hydrochloric acid (HCl, 37%, Aldrich) were additionally employed for the synthesis of large crystals of HKUST-1. DDW, methanol (MeOH, 99.5%, Daejung), EtOH, DMF, phenol (C_6H_5OH, PhOH, 99.0-100.5%, Aldrich), toluene ($C_6H_5CH_3$, Tol, 99.8%, Alfa), deuterated trichloromethane ($CDCl_3$, TCM-d, 99%, Aldrich), and deuterated toluene ($C_6D_5CD_3$, Tol-d_8, 99%, Alfa) were used for the in situ and ex situ ^{1}H nuclear magnetic resonance (^{1}H NMR) spectroscopic analyses. Before the ^{1}H NMR experiments, all the chemicals except DDW were purified with zeolite 4A in a moisture-free argon-filled glove box to remove water in the solvents. Basolite C300 ($Cu_3(BTC)_2$, Aldrich), acetophenone ($C_6H_5COCH_3$, 99.0%, Aldrich), acetone (99.5%, Daejung), phenyl silane ($C_6H_5SiH_3$, 97.0%, Aldrich), DMF, acetonitrile (MeCN, 99.8%, Aldrich), diethyl ether (Et_2O, DEE, 99.0%, Aldrich), trichloromethane ($CHCl_3$, TCM, 99.0%, Alfa), dichloromethane (CH_2Cl_2, DCM, 99.5%, Daejung), chlorobenzene (C_6H_5Cl, PhCl, 99.0%, Alfa), and Tol were used for the catalytic hydrogenation reaction of the acetophenone and acetone. Basolite C300 powder was activated under vacuum at 150 °C to remove water and solvent molecules inside the pores before use, and all chemical reagents were purified with zeolite 4A prior to examining the catalytic reactions. Deuterated sulfuric acid (D_2SO_4, 96-98 wt% in D_2O, 99.5 atomic % in deuterium, Aldrich) was used to digest HKUST-1 crystals before checking the samples' chemical purities with the ^{1}H NMR spectroscopic analysis. Before use, all the synthesized MOFs were stored in a moisture-free argon-filled glove box.

Synthesis of small HKUST-1 crystal (averagely 10 μm). We synthesized small HKUST-1 crystals following the procedure described in our previous reports.[1-4] Briefly, $Cu(NO_3)_2 \cdot 2.5H_2O$ (0.87 g, 3.6 mmol) was dissolved in 10 mL of DDW in a vial. H_3BTC (0.22 g, 1.0 mmol) was dissolved in 10 mL of EtOH using a separate vial. The $Cu(NO_3)_2$ solution was quickly added to the vial containing the H_3BTC solution. After the mixed solution was continuously stirred for 10 min at room temperature, 1 mL of DMF was added to the mixture. Then, the vial was sealed with polytetrafluoroethylene (PTFE) tape, and the sealed vial was placed in an oven at 80 °C for 20 h to allow the mixture to react. After the product cooled to room temperature, we collected and washed the crystals (pristine HKUST-1) with a mixed solvent of H_2O and EtOH.

Synthesis of large HKUST-1 crystal (averagely 400 μm). Large HKUST-1 crystals were synthesized with a similar procedure described above except using $CuCl_2$ instead of $Cu(NO_3)_2$ and adding HCl. $CuCl_2 \cdot 2H_2O$ (1.47 g, 8.6 mmol) was dissolved in 200 mL of DDW in a glass bottle. Then, 2.20 g of DMF was added to the $CuCl_2$ solution. After H_3BTC (2.10 g, 10 mmol) was dissolved in 200 mL of EtOH in a separate glass bottle, 0.25 g of HCl was added to the H_3BTC solution. Then, the $CuCl_2$ solution was quickly added to the bottle containing the H_3BTC solution. After the bottle was sealed with a polypropylene cap, the bottle was placed in an oven at 80 °C for 5 d. After the product cooled to room temperature, we collected and washed the pristine large HKUST-1 crystals with a mixed solvent of H_2O and EtOH.

Thermal activation of HKUST-1. Pristine HKUST-1 crystals were thermally activated to remove the coordinated and pore-filling H_2O and EtOH molecules from the crystals before performing in situ and ex situ ^{1}H NMR measurements. A pristine HKUST-1 sample was placed in a glass vacuum tube. Then, the tube was heated at 180 °C for 20 h under vacuum (~10^{-3} Torr) conditions. After the activation, the tubes were transferred into a moisture-free Ar-charged glovebox prior to use. Basolite C300 powder

was also thermally activated with a similar method under vacuum at 150 °C before the catalytic hydrogenation reactions were performed.

In situ ^{1}H NMR measurements. In order to measure the in situ ^{1}NMR spectra of water-containing TCM-d (H_2O@TCM-d) with large activated HKUST-1 (Act-HKUST-1) crystals, 4 mL of TCM-d was placed in a vial, then, 3.56 μL of H_2O, which amount is stoichiometric to the number of open metal sites in 20 mg of HKUST-1 crystals, was added into the vial. We transferred the solvent into two NMR tubes separately with 2 mL respectively; one was for the in situ ^{1}H NMR with large Act-HKUST-1 crystals, and the other was for analyzing the initial quantity of H_2O in the H_2O@TCM-d for comparison. After introducing 20 mg of large Act-HKUST-1 crystals (averagely 400 μm) into an NMR tube, we measured the in situ ^{1}H NMR spectra of H_2O@TCM-d solvent with Act-HKUST-1 crystals, increasing and decreasing the temperature at 25 °C, 40 °C, and 55 °C. We separately measured a ^{1}H NMR spectrum of the H_2O@TCM-d without Act-HKUST-1 crystals to quantify the initial amount of H_2O molecules in the H_2O@TCM-d at 25 °C. In situ ^{1}H NMR spectra of MeOH-, EtOH-, DMF-, MeCN-, PhOH-, and Tol-included TCM-d (MeOH@TCM-d, EtOH@TCM-d, DMF@TCM-d, MeCN@TCM-d, PhOH@TCM-d, and Tol@TCM-d, respectively) with small HKUST-1 crystals (averagely 10 μm) were also taken with the same method described above except using small HKUST-1 crystals. Before measurements, we prepared H_2O-, MeOH-, EtOH-, DMF-, MeCN-, PhOH-, and Tol-containing TCM-d solvents (H_2O@TCM-d, MeOH@TCM-d, EtOH@TCM-d, DMF@TCM-d, MeCN@TCM-d, PhOH@TCM-d, and Tol@TCM-d, respectively) by adding 3.54 μL of H_2O, 8.00 μL of MeOH, 11.58 μL of EtOH, 10.32 μL of MeCN, 15.24 μL of DMF, 18.62 mg of PhOH, and 20.94 μL of Tol into the 4 mL of TCM-d solvent. A control experiment with PhOH-containing Tol-d_8 (PhOH@Tol-d_8) was also performed by adding 18.62 mg of PhOH into 4 mL of Tol-d_8 solvent. Before use, all solvents except water (DDW) were purified with zeolite 4A in a moisture-free Ar-charged glovebox, and all samples were prepared in the glovebox.

Ex-situ ^{1}H NMR measurements. To measure the ex-situ ^{1}NMR spectra of the H_2O@TCM-d with small Act-HKUST-1 crystals, we prepared the H_2O@TCM-d solvent by adding 14.44 μL of H_2O to 16 mL of TCM-d in a vial. We transferred the solvent into six NMR tubes separately with approximately 2.5 mL respectively; five vials were for the ex situ ^{1}H NMR with Act-HKUST-1 crystals, and the last one was for analyzing the initial quantity of H_2O in the H_2O@TCM-d for comparison. After introducing 20 mg of small Act-HKUST-1 crystals into an NMR tube, we placed the vial in an oil bath controlled at 25 °C on a hot plate. After 1 hour, we transferred 2 ml of the supernatant solution to an NMR tube from the vial. The ex-situ ^{1}H NMR experiments at 40 and 55 °C were performed with the same method. Meanwhile, the initial quantity of H_2O in the H_2O@TCM-d was analyzed after transferring the authentic H_2O@TCM-d into an NMR tube. The ex-situ ^{1}H NMR spectra of MeOH@TCM-d, EtOH@TCM-d, DMF@TCM-d, PhOH@TCM-d, and Tol@TCM-d samples were obtained following the procedure described above. For the experiments, we prepared the MeOH@TCM-d, EtOH@TCM-d, DMF@TCM-d, PhOH@TCM-d, and Tol@TCM-d solvents by adding 32.18 μL of MeOH, 46.27 μL of EtOH, 61.03 μL of DMF, 74.45 mg of PhOH, and 83.84 μL of Tol into 16 mL of TCM-d, respectively. The entire process above was conducted under an inert atmosphere of a moisture-free Ar-charged glovebox.

Measurement of Raman spectra. We measured H_2O-, MeOH-, EtOH-, DMF-, MeCN-, PhOH-, DCM-, TCM-, and Tol-coordinating HKUST-1 crystals (hereafter denoted as H_2O-HKUST-1, MeOH-HKUST-1, EtOH-HKUST-1, DMF-HKUST-1, MeCN-HKUST-1, PhOH-HKUST-1, DCM-HKUST-1, TCM-HKUST-1, and Tol-HKUST-1, respectively, where HKUST-1 = completely desolvated HKUST-1). To this end, we prepared MeOH-HKUST-1, EtOH-HKUST-1, DMF-HKUST-1, MeCN-HKUST-1, and PhOH-HKUST-1 samples by soaking 50 mg of large Act-HKUST-1 crystals into the corresponding solvent, respectively. Then, we transferred the crystal samples into disc-shaped quartz cells (Starna, Type 37GS Cylindrical Cells with

Quartz to Borofloat graded seal) after slightly drying the crystals. To prepare DCM-HKUST-1, TCM-HKUST-1, and Tol-HKUST-1 samples, we transferred large Act-HKUST-1 crystals into the disc-shaped quartz cells and introduced the corresponding solvents in the quartz cells, respectively. H_2O-HKUST-1 sample was prepared by exposing the large Act-HKUST-1 crystals to water vapour with the '*vial-in-vial*' method, where a smaller vial containing the Act-HKUST-1 crystals is placed in a capped larger vial containing DDW. Then, the crystals were transferred into the disc-shaped quartz cells before taking the Raman spectrum. The entire process described above was conducted under an inert atmosphere of an Ar-charged glovebox.

Measurement of UV-vis absorption spectra. To take the UV-vis absorption spectrum of Act-HKUST-1, we transferred 65 mg of small Act-HKUST-1 crystals into disc-shaped quartz cells. Subsequently, the cell was sealed with a glass cork using grease (Apiezon, H high-temperature vacuum greases). UV-vis absorption spectra of H_2O-HKUST-1 crystals in TCM were taken after introducing purified TCM solvent into an H_2O-HKUST-1-containing quartz cell before sealing. Before taking the absorption spectra, we controlled the temperatures of the cell at 25 and 55 °C. All sample preparation were performed under an inert atmosphere of an Ar-charged glovebox.

Sample purity check with ^{1}H NMR measurements. Phase and chemical purities of all Raman samples were checked by measuring powder X-ray diffraction (PXRD) patterns and ^{1}H NMR spectra, respectively. To check the chemical purities, we introduced a tiny amount of corresponding HKUST-1 crystals into an NMR tube containing 0.5 mL of D_2SO_4 and thoroughly digested the crystals. This preparation was conducted in an Ar-charged glove box. The NMR tubes were kept sealed with plastic caps and acrylic Parafilm® prior to being taken out from the glove box. The PXRD patterns of the samples were recorded after Raman measurements.

Catalytic hydrogenation reaction of acetophenone and acetone. 40 mg of activated Basolite C300 powder (Act-HKUST-1) were introduced in a vial containing 2 mL of dried DMF solvent. After 93.5 µL (1.00 mmol) of acetophenone and 295.8 µL (3.00 mmol) of phenylsilane were added to the vial, the vial was continuously stirred for 5, 15, 30, and 60 min, respectively, at 25 °C. Then, we transferred the supernatant solution into an NMR tube to analyze the conversion efficiency. The above process was conducted under an inert atmosphere of a moisture-free Ar-charged glovebox. We examined MeCN, DEE, TCM, DCM, PhCl, and Tol solvents for comparison with the same method described above. The hydrogenation reactions of acetone in the solvents with Act-HKUST-1 crystals were also tested with the same procedure except for using acetone instead of acetophenone. The hydrogenations of acetone and acetophenone without Act-HKUST-1 were also examined for comparison.

Instrumentation. DDW was obtained from a water purification system (Merck Millipore, MQ Direct 8). Diffuse reflectance UV-vis absorption spectra of the samples were recorded using an Agilent Cary 5000 UV-VIS-NIR spectrophotometer. PXRD patterns were obtained using a PANalytical diffractometer (Empyrean) with a monochromatic nickel-filtered Cu K_α beam. ^{1}H-NMR spectra were recorded using an AVANCE III HD FT-NMR spectrometer (Bruker, 400 MHz for ^{1}H). The ^{1}H chemical shifts were referenced to the residual proton resonance of the solvent. Raman spectra were recorded using a Nicolet Almega XR dispersive Raman spectrometer (Thermo Scientific). Single crystal X-Ray diffraction data was collected in D8 Venture (Bruker) equipped with a Mo X-ray tube (Kα1 = 0.7107 Å, 50 kV, and 30 mA).

Section S2. Unsaturated diffuse-reflectance UV-vis absorption spectra

An insightful reviewer asked us to measure the unsaturated diffuse-reflectance UV-vis absorption spectra on the Agilent Cary 5000. To obtain the unsaturated spectra, we have measured the spectra after diluting the HKUST-1 powder samples with aluminum oxide (Al_2O_3) white powder that does not absorb light in the UV-vis-near IR region.

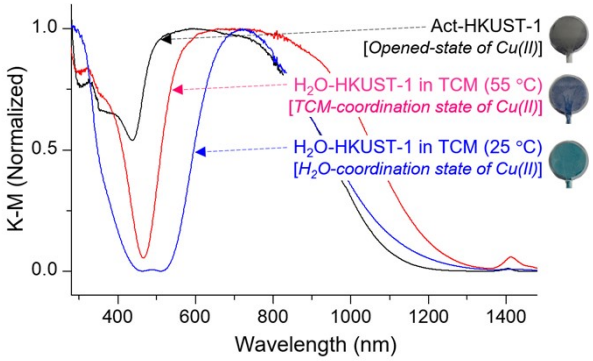

Fig. S1 Diffuse-reflectance UV-vis absorption spectra of Act-HKUST-1 (black curve) and TCM-wet H_2O-HKUST-1 crystalline powders at 25 and 55 °C (blue and pink curves, respectively). Inset (right) shows photograph images of disc-shaped quartz cells containing Act-HKUST-1 and H_2O-HKUST-1 crystals under corresponding conditions.

Section S3. Optical and scanning electron microscope images of HKUST-1 crystals

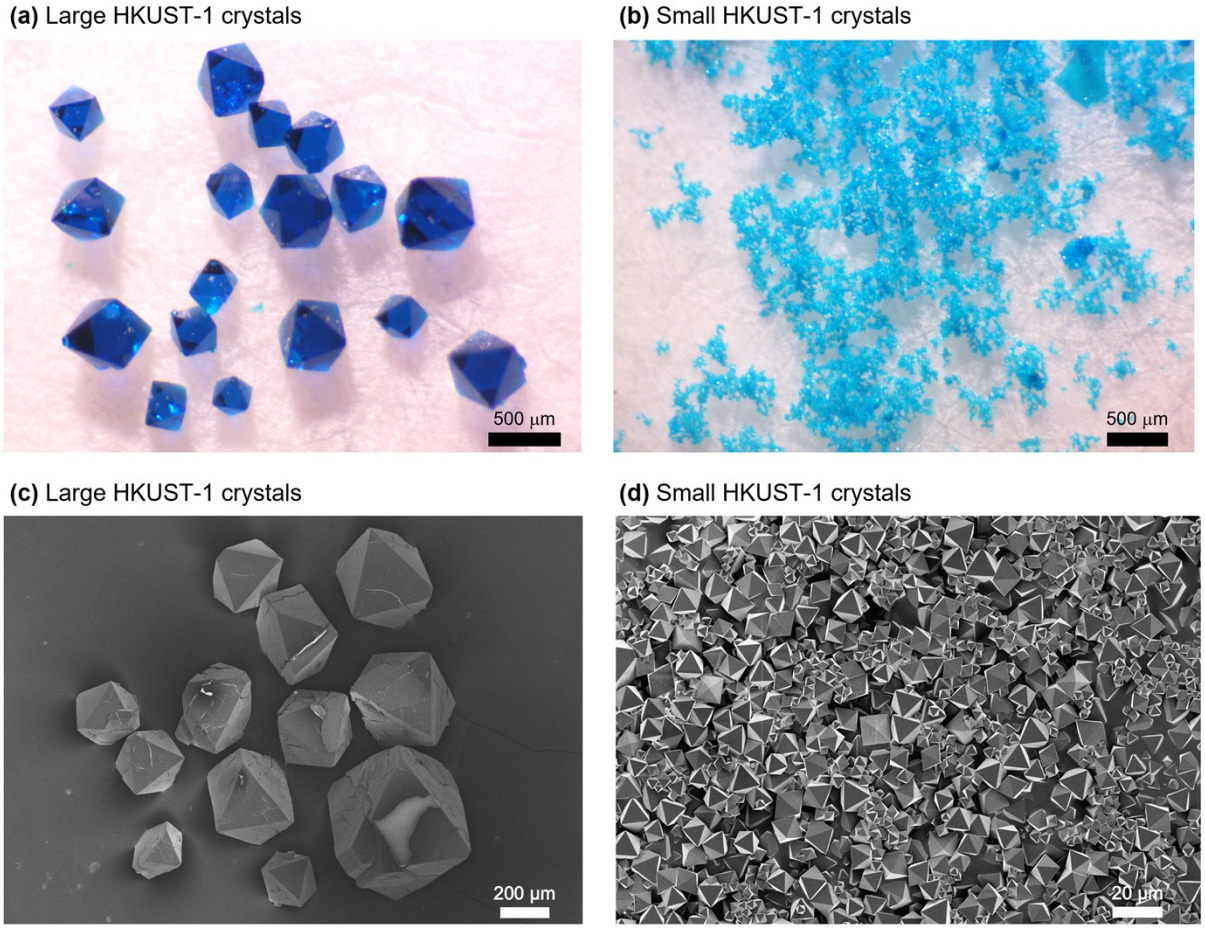

Fig. S2 (a, b) Optical microscope and (c, d) scanning electron microscope (SEM) images of (a, c) large and (b, d) small HKUST-1 crystals that have averagely 400 and 10 μm sizes.

Section S4. In situ ^{1}H NMR spectra recorded with large HKUST-1 crystals

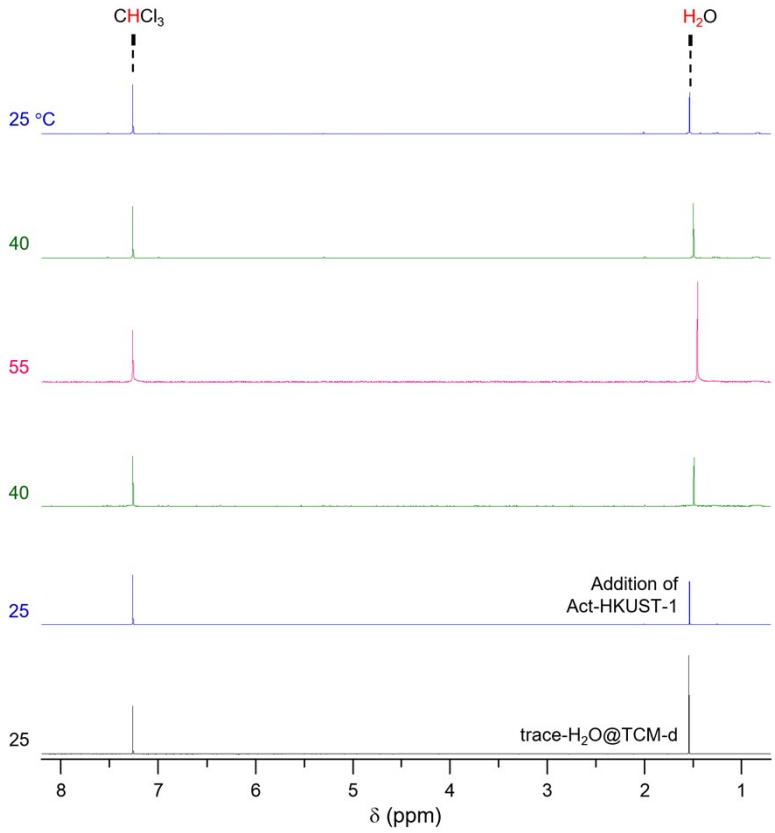

Fig. S3 Broad view of in situ ^{1}H NMR spectra of H_2O molecules in H_2O@TCM-d solvent measured with large Act-HKUST-1 crystals (ca. 200-500 μm) at 25 °C (blue curves), 40 °C (green curves), and 55 °C (red curve), increasing and decreasing the temperatures. ^{1}H NMR spectrum of H_2O@TCM-d without Act-HKUST-1 crystals (black curve) was also measured for comparison.

Section S5. ^{1}H NMR spectra of pure H_2O, MeOH, and EtOH in TCM-d solvent at different temperatures

One might wonder whether the chemical shifts of hydroxy protons in H_2O, MeOH, and EtOH would alter depending on temperatures. We conducted control experiments with pure H_2O, MeOH, and EtOH solvents (without HKUST-1 crystals) at 25, 40, and 55 °C to address this question. As a result, we observed that the chemical shifts of the hydroxy protons are highly dependent upon the temperatures, as seen in the in situ ^{1}H NMR spectra below.

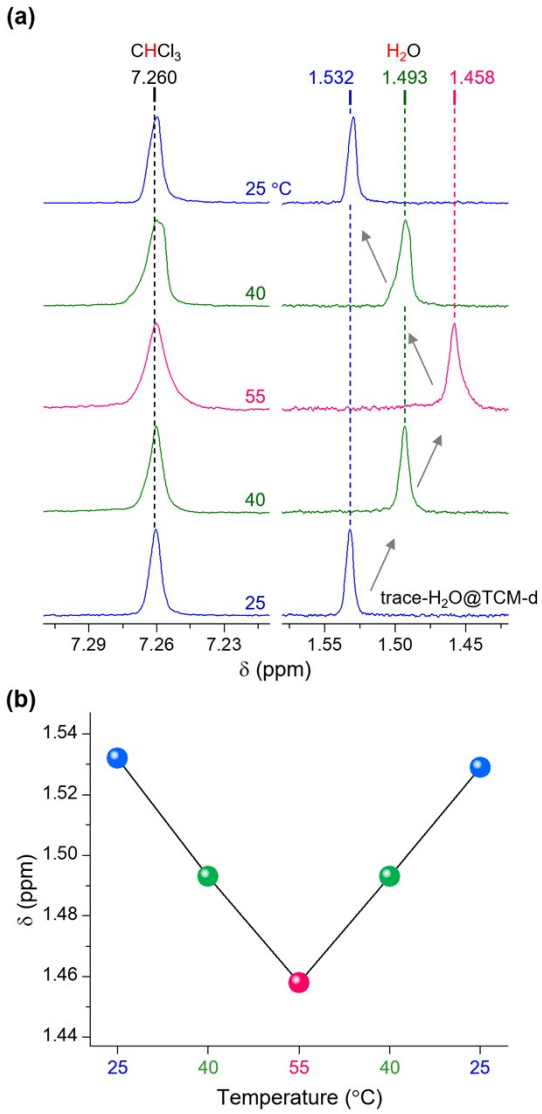

Fig. S4 (a) ^{1}H NMR spectra of pure H_2O molecules in H_2O@TCM-d solvent measured at 25 °C (blue curves), 40 °C (green curves), and 55 °C (red curve), increasing and decreasing the temperatures. (b) Plots for the in situ chemical shifts of the protons of pure H_2O recorded in the ^{1}H NMR spectra of H_2O@TCM-d.

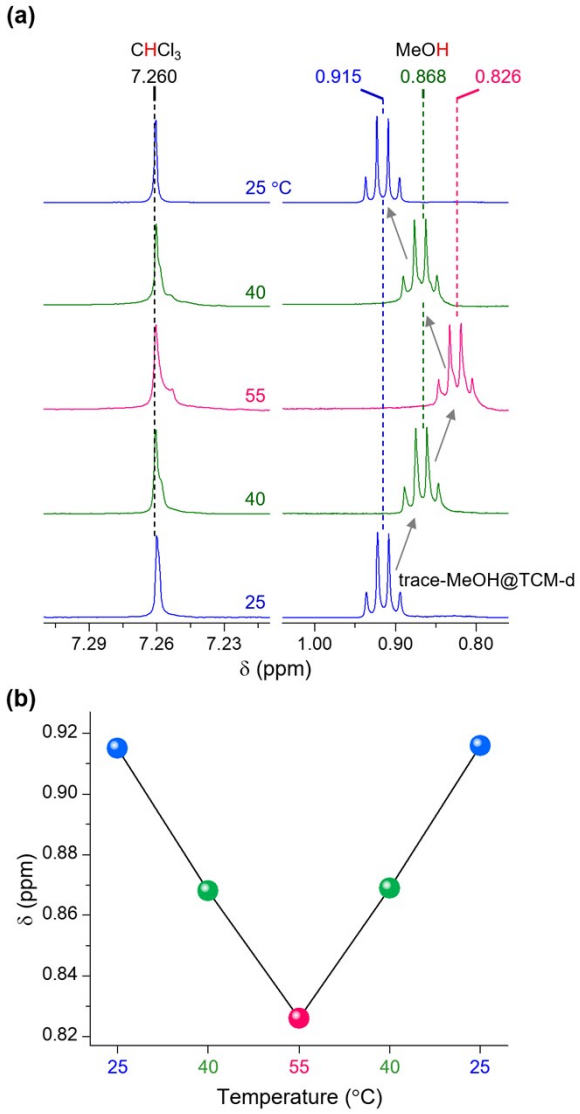

Fig. S5 (a) ^{1}H NMR spectra of pure MeOH molecules in MeOH@TCM-d solvent measured at 25 °C (blue curves), 40 °C (green curves), and 55 °C (red curve), increasing and decreasing the temperatures. (b) Plots for the in situ chemical shifts of the hydroxy proton of pure MeOH recorded in the ^{1}H NMR spectra of MeOH@TCM-d.

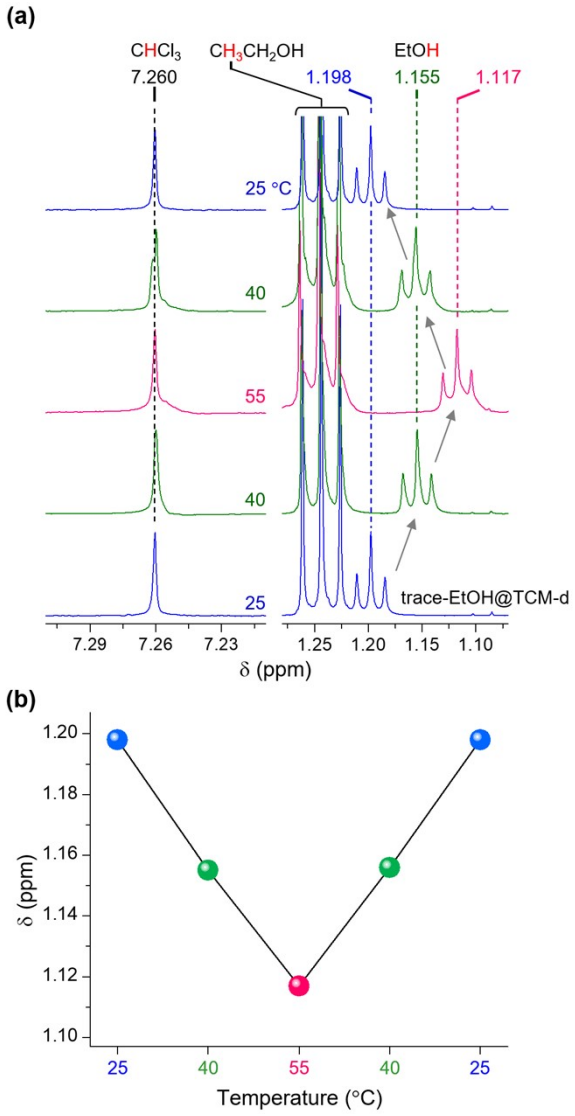

Fig. S6 (a) ^{1}H NMR spectra of pure EtOH molecules in EtOH@TCM-d solvent measured at 25 °C (blue curves), 40 °C (green curves), and 55 °C (red curve), increasing and decreasing the temperatures. (b) Plots for the in situ chemical shifts of the hydroxy proton of pure EtOH recorded in the ^{1}H NMR spectra of EtOH@TCM-d.

Section S6. In situ ^{1}H NMR spectra recorded with small HKUST-1 crystals

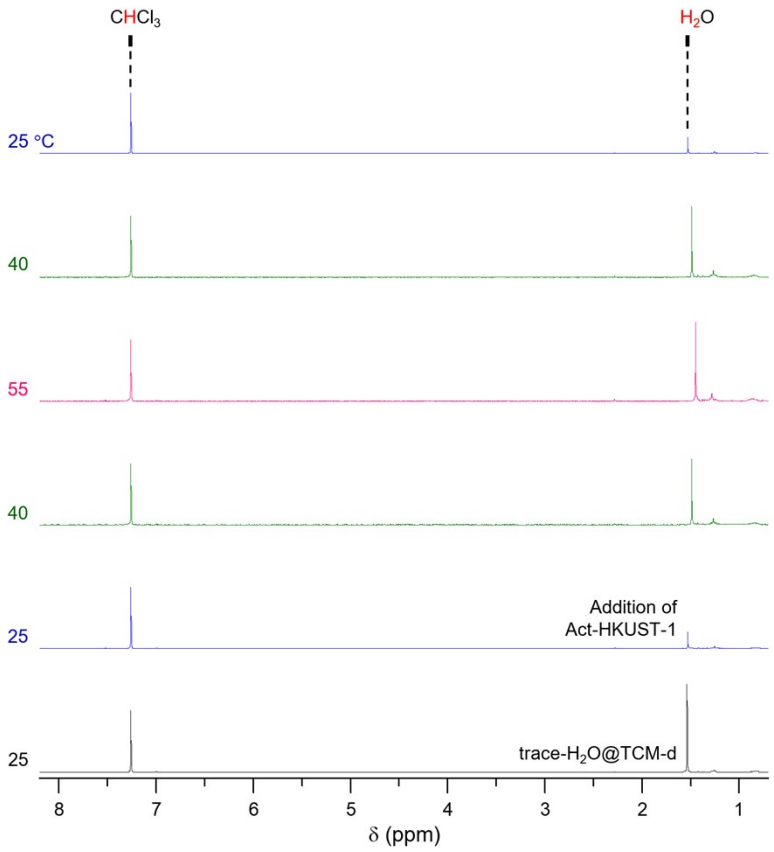

Fig. S7 Broad view of in situ ^{1}H NMR spectra of H_2O molecules in H_2O@TCM-d solvent measured with small Act-HKUST-1 crystals (ca. 10 μm) at 25 °C (blue curves), 40 °C (green curves), and 55 °C (red curve), increasing and decreasing the temperatures. ^{1}H NMR spectrum of H_2O@TCM-d without Act-HKUST-1 crystals (black curve) was also measured for comparison.

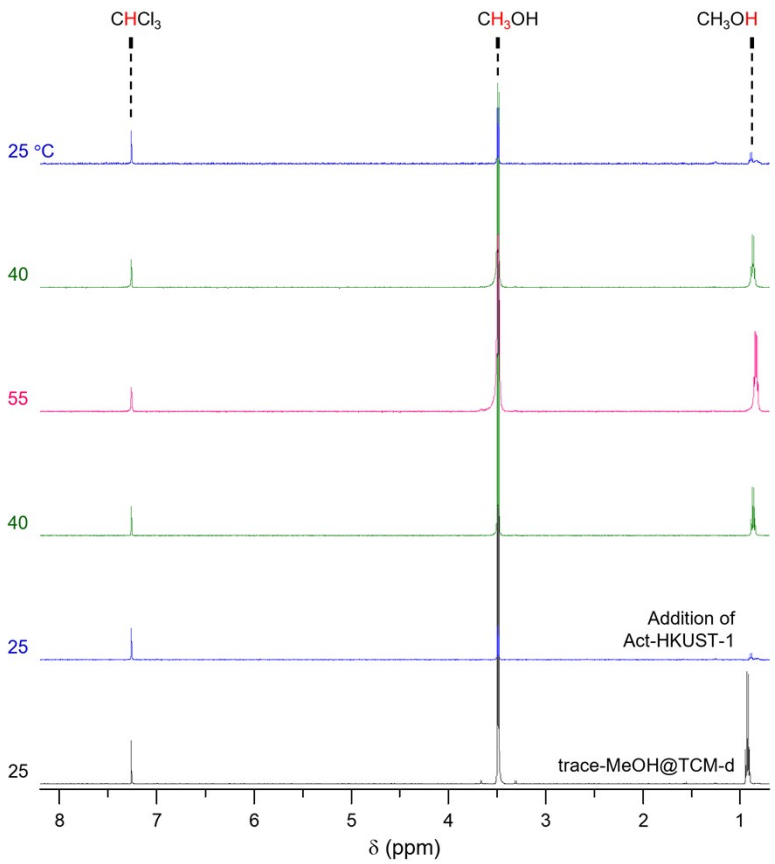

Fig. S8 Broad view of in situ ^{1}H NMR spectra of MeOH molecules in MeOH@TCM-d solvent measured with small Act-HKUST-1 crystals (ca. 10 μm) at 25 °C (blue curves), 40 °C (green curves), and 55 °C (red curve), increasing and decreasing the temperatures. ^{1}H NMR spectrum of MeOH@TCM-d without Act-HKUST-1 crystals (black curve) was also measured for comparison.

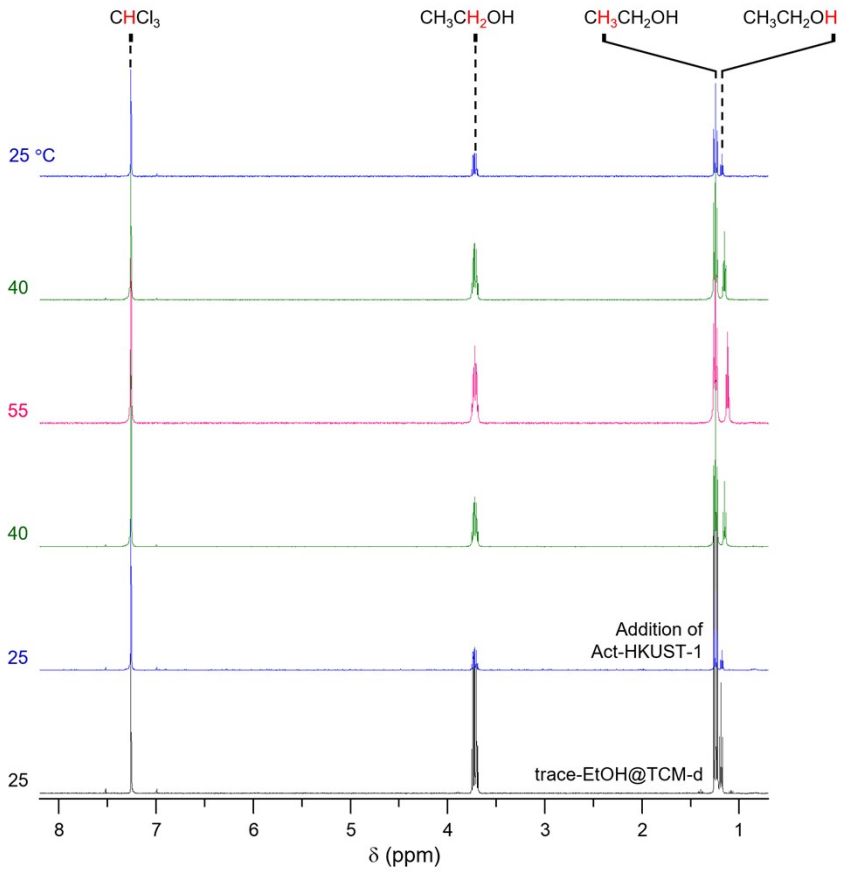

Fig. S9 Broad view of in situ ^{1}H NMR spectra of EtOH molecules in EtOH@TCM-d solvent measured with small Act-HKUST-1 crystals (ca. 10 μm) at 25 °C (blue curves), 40 °C (green curves), and 55 °C (red curve), increasing and decreasing the temperatures. ^{1}H NMR spectrum of EtOH@TCM-d without Act-HKUST-1 crystals (black curve) was also measured for comparison.

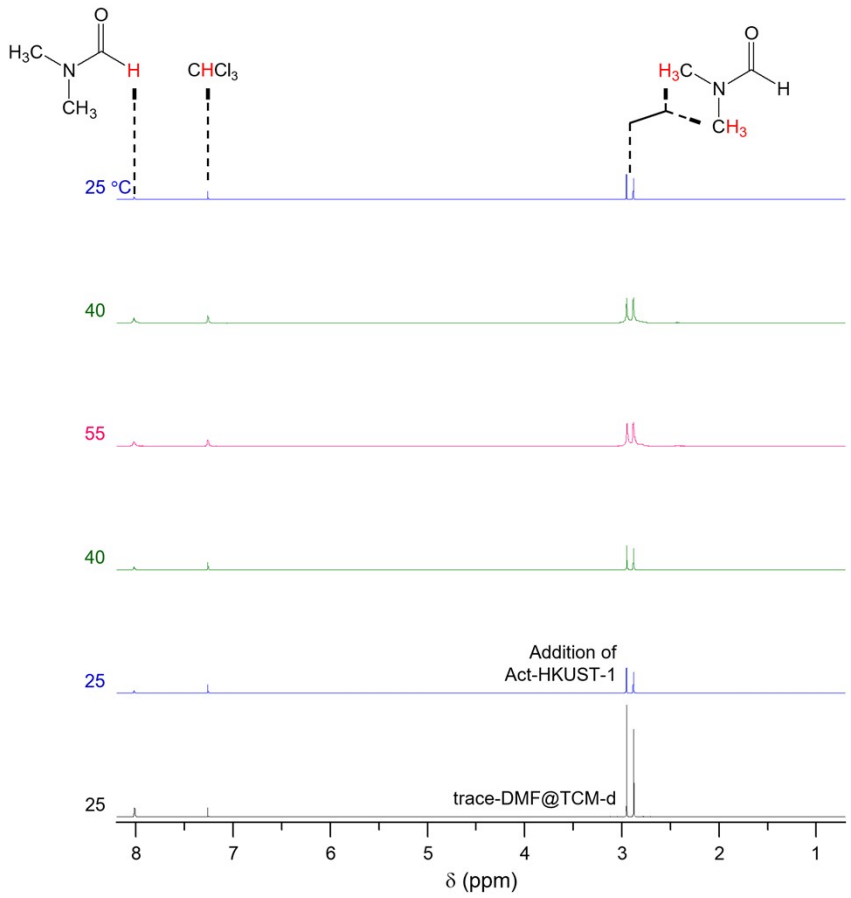

Fig. S10 Broad view of in situ ^{1}H NMR spectra of DMF molecules in DMF@TCM-d solvent measured with small Act-HKUST-1 crystals (ca. 10 μm) at 25 °C (blue curves), 40 °C (green curves), and 55 °C (red curve), increasing and decreasing the temperatures. ^{1}H NMR spectrum of DMF@TCM-d without Act-HKUST-1 crystals (black curve) was also measured for comparison.

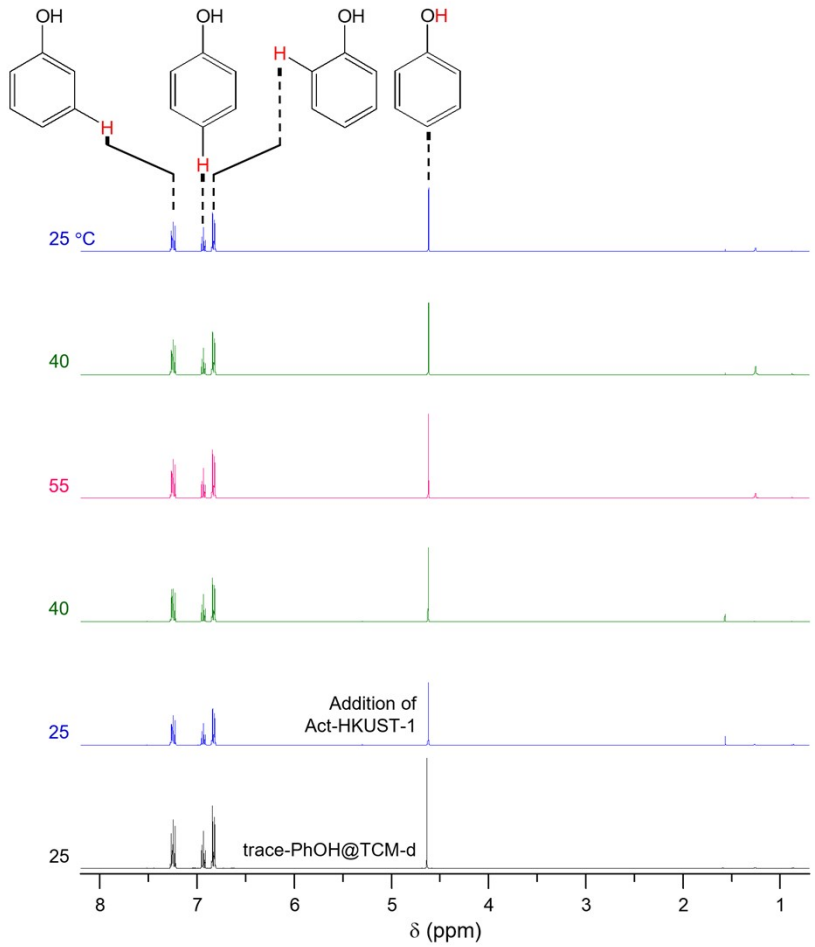

Fig. S11 Broad view of in situ ^{1}H NMR spectra of PhOH molecules in PhOH@TCM-d solvent measured with small Act-HKUST-1 crystals (ca. 10 μm) at 25 °C (blue curves), 40 °C (green curves), and 55 °C (red curve), increasing and decreasing the temperatures. ^{1}H NMR spectrum of PhOH@TCM-d without Act-HKUST-1 crystals (black curve) was also measured for comparison.

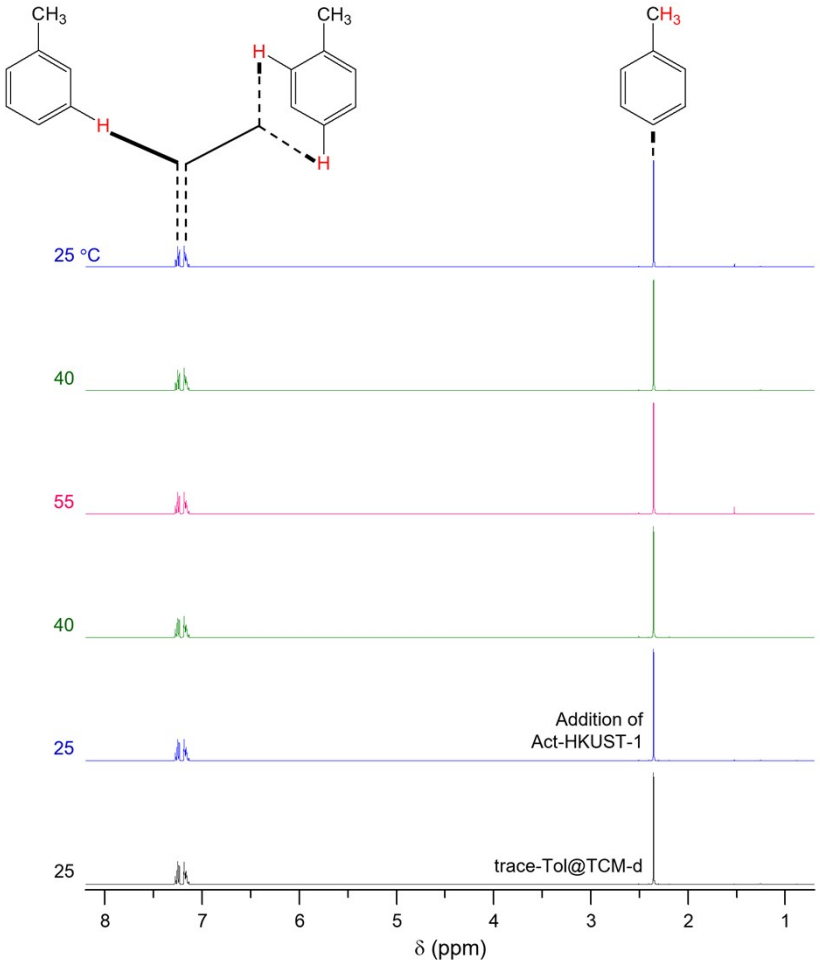

Fig. S12 Broad view of in situ ^{1}H NMR spectra of toluene molecules in Tol@TCM-d solvent measured with small Act-HKUST-1 crystals (ca. 10 μm) at 25 °C (blue curves), 40 °C (green curves), and 55 °C (red curve), increasing and decreasing the temperatures. ^{1}H NMR spectrum of Tol@TCM-d without Act-HKUST-1 crystals (black curve) was also measured for comparison.

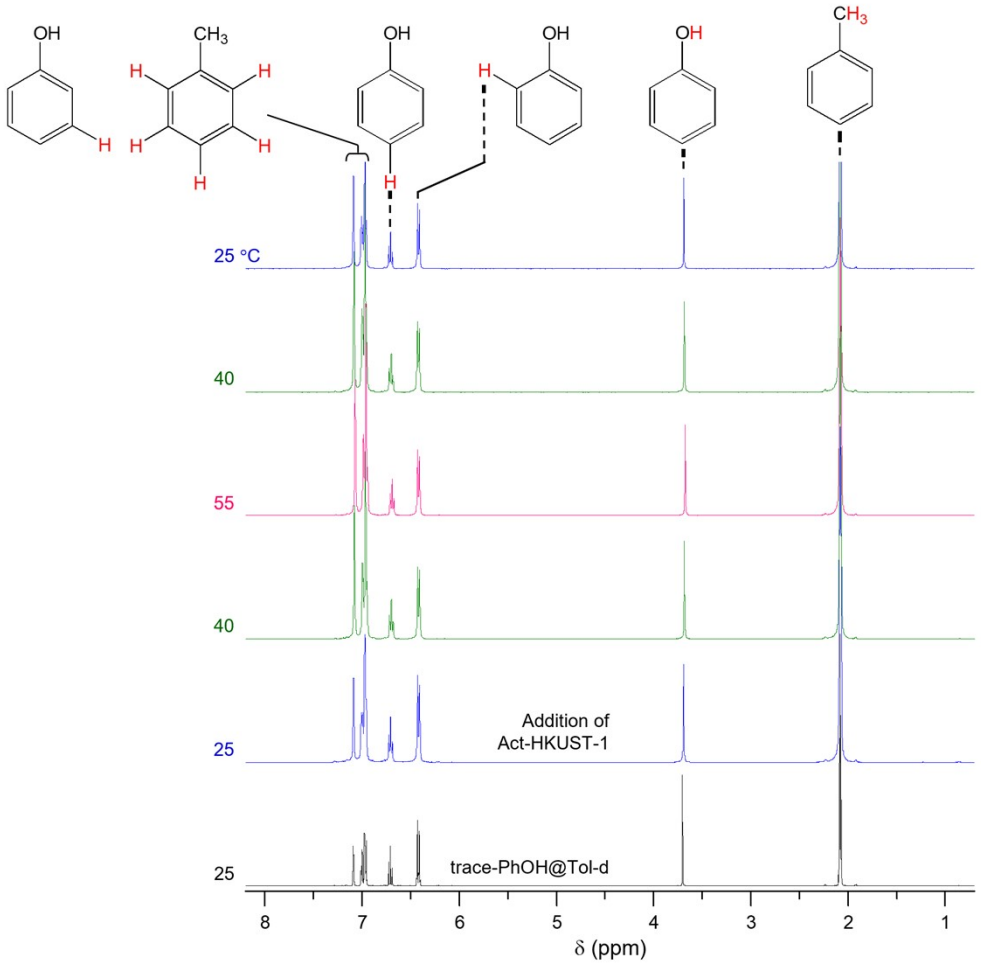

Fig. S13 Broad view of in situ ^{1}H NMR spectra of PhOH molecules in PhOH@Tol-d_8 solvent measured with small Act-HKUST-1 crystals (ca. 10 μm) at 25 °C (blue curves), 40 °C (green curves), and 55 °C (red curve), increasing and decreasing the temperatures. ^{1}H NMR spectrum of PhOH@Tol-d_8 without Act-HKUST-1 crystals (black curve) was also measured for comparison.

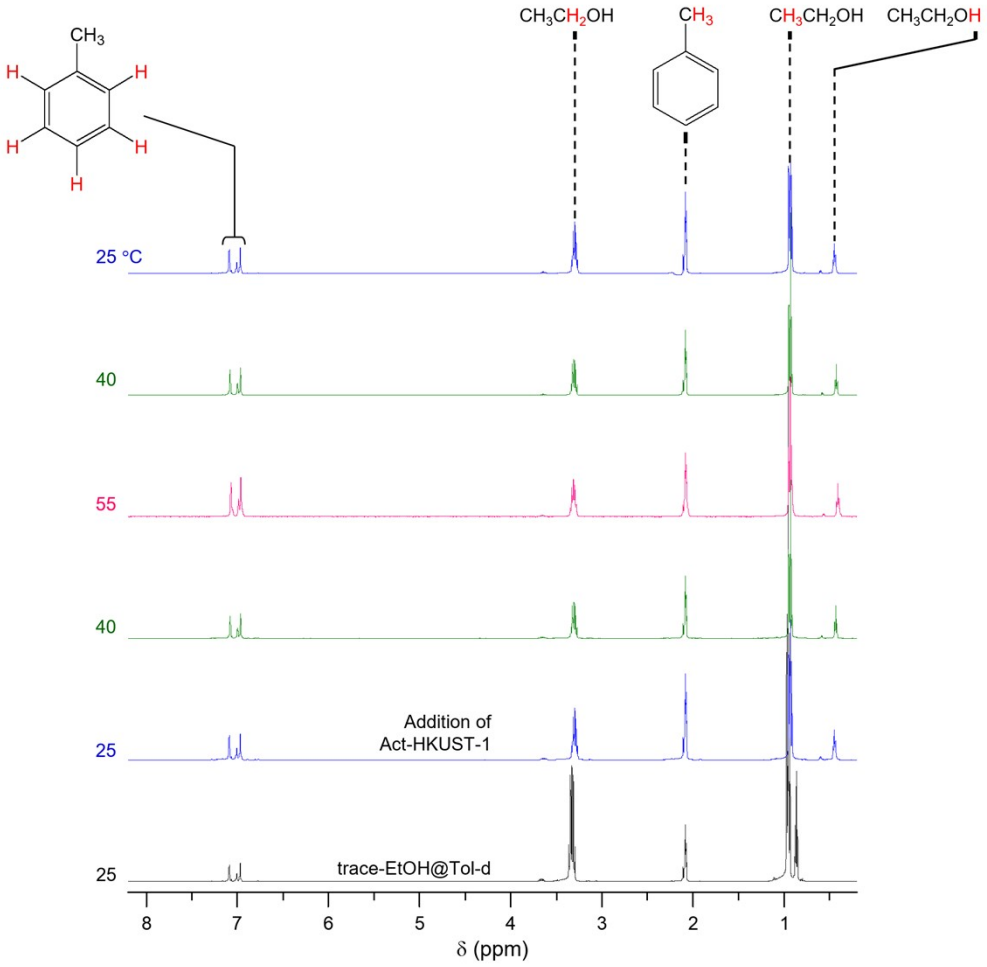

Fig. S14 Broad view of in situ ^{1}H NMR spectra of EtOH molecules in EtOH@Tol-d_8 solvent measured with small Act-HKUST-1 crystals (ca. 10 μm) at 25 °C (blue curves), 40 °C (green curves), and 55 °C (red curve), increasing and decreasing the temperatures. ^{1}H NMR spectrum of EtOH@Tol-d_8 without Act-HKUST-1 crystals (black curve) was also measured for comparison.

Section S7. In situ ^{1}H NMR spectra recorded with MeCN@TCM-d solvent

Another insightful reviewer asked us about dynamic coordinative equilibrium in MeCN@TCM-d solvent. To address this question, we have measured in situ ^{1}H NMR spectra with MeCN@TCM-d. When we placed the Act-HKUST-1 in the MeCN@TCM-d, the integral value of MeCN in the TCM-d solvent decreased to 0.336, indicating approximately 66% coordination of MeCN at the paddlewheel Cu(II) centers. However, the value remained unchanged during the temperature variation by 55 °C. This implies that MeCN is strongly coordinated at the Cu(II) center.

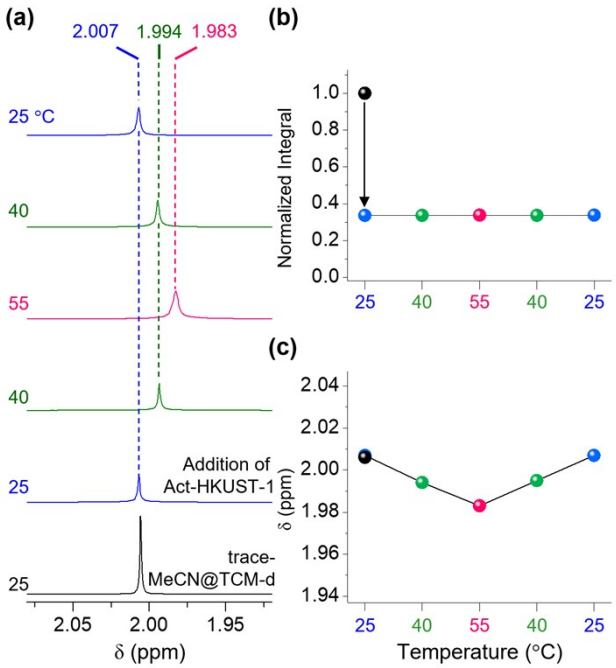

Fig. S15 (a) In situ ^{1}H NMR spectra of MeCN in MeCN@TCM-d measured with small Act-HKUST-1 crystals (ca. 10 μm) at 25 °C (blue curve), 40 °C (green curve), and 55 °C (red curve), increasing and decreasing the temperatures. ^{1}H NMR spectrum of MeCN@TCM-d without Act-HKUST-1 crystals (black curve) was also measured for comparison. (b and c) Plots for (b) the normalized integrals and (c) the chemical shifts of the MeCN proton peaks obtained from the in situ ^{1}H NMR spectra of MeCN@TCM-d with respect to the temperatures. The integral values were calibrated with the residual TCM ($CHCl_3$) in TCM-d ($CDCl_3$).

Section S8. In silico simulation for the sizes of Lewis-base molecules

One might wonder how many Lewis-base (LB) molecules could coordinate at OMSs in a unit cell. To address the question, we simulated the sizes of LB molecules, including H_2O, MeOH, EtOH, DMF, PhOH, and TCM. We also simulate the size of the large cage of HKUST-1. As a result, we found that while small molecules such as H_2O, MeOH, and EtOH can coordinate at all OMSs (12 sites in a unit cell), larger molecules such as DMF, PhOH, and TCM can coordinate 6, 4, and 6 sites in a unit cell, respectively.

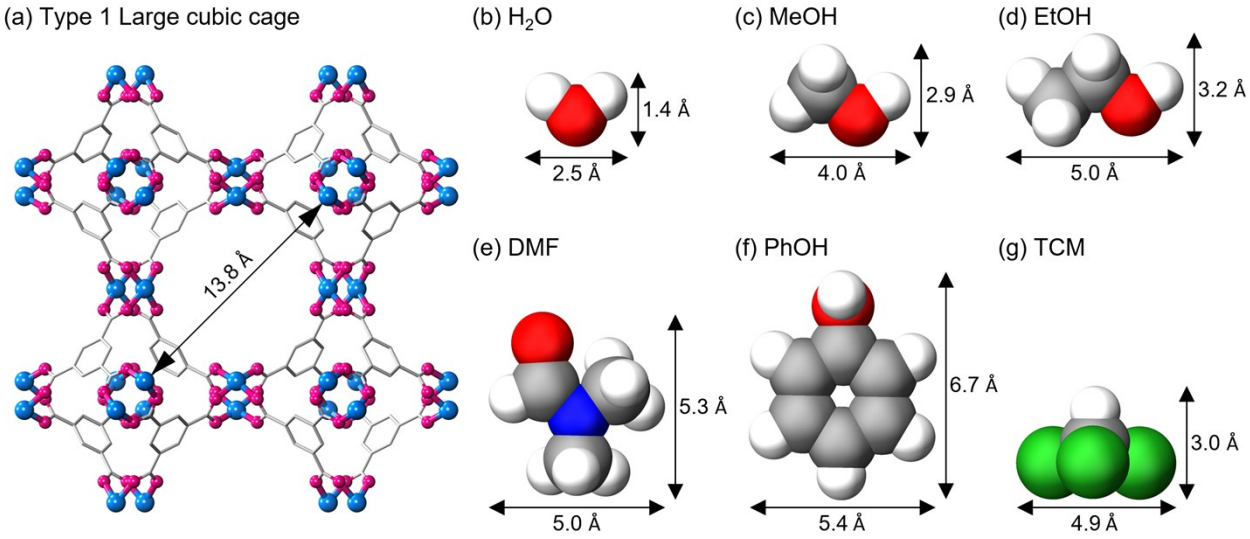

Fig. S16 In silico simulation for the sizes of (a) HKUST-1 large pore and (b-g) Lewis-base molecules of (b) H_2O, (c) MeOH, (d) EtOH, (e) DMF, (f) PhOH, and (g) TCM.

Section S9. Ex-situ ^{1}H NMR spectra recorded with small HKUST-1 crystals

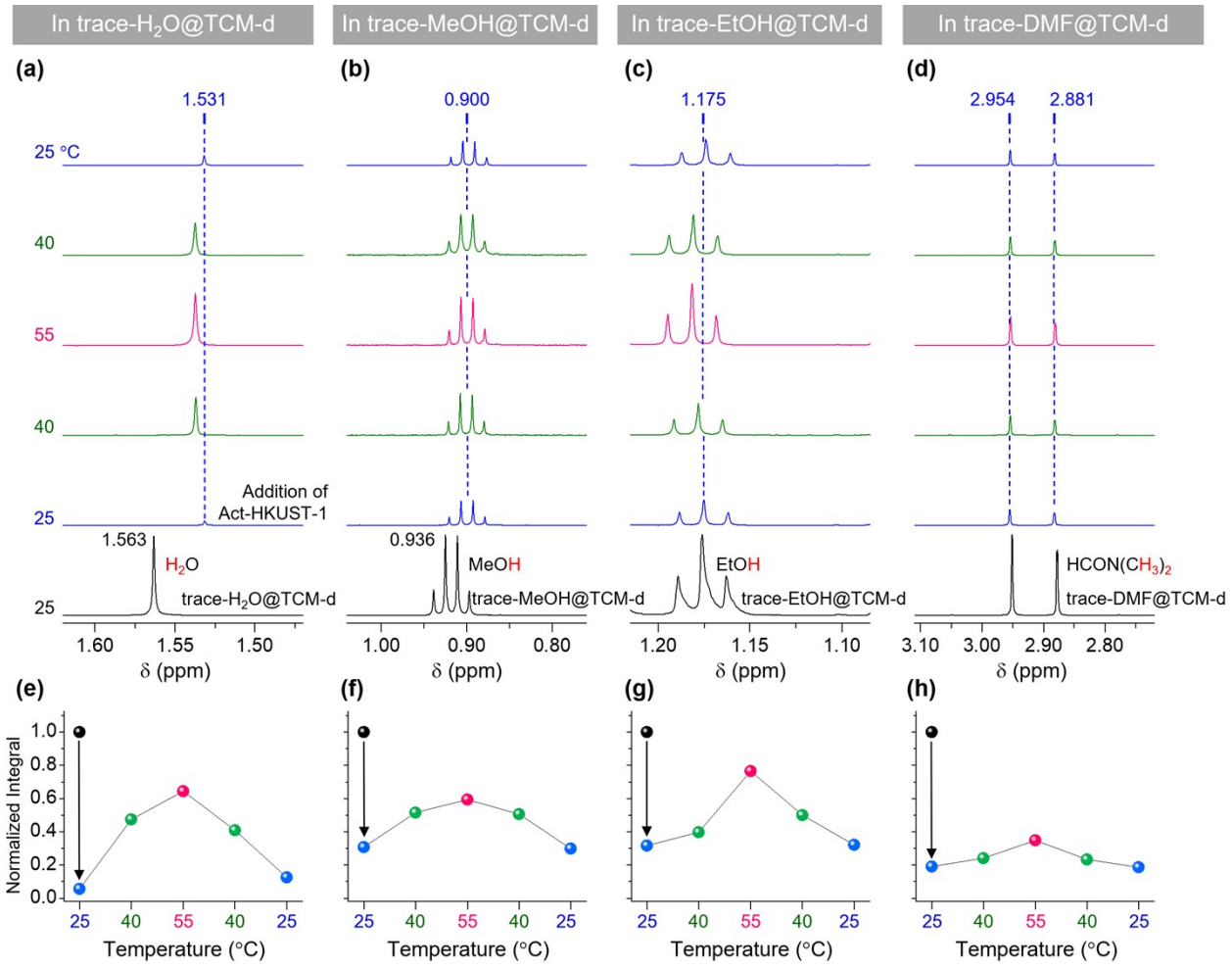

Fig. S17 (a-d) Ex-situ ^{1}H NMR spectra and (e-h) integral profiles of (a, e) H_2O in H_2O@TCM-d, (b, f) MeOH in MeOH@TCM-d, (c, g) EtOH in EtOH@TCM-d, and (d, h) DMF in DMF@TCM-d measured at a fixed temperature of 25 °C, after taking corresponding supernatant solvents from each vial containing small Act-HKUST-1 crystals (ca. 10 μm), which was placed in a temperature-controlled oil bath at 25 °C (blue curves), 40 °C (green curves), and 55 °C (red curves), respectively. Note that the chemical shifts of H_2O, MeOH, EtOH, and DMF do not alter due to the fixed temperature (25 °C) of the NMR tube specimen. ^{1}H NMR spectra of (a) H_2O@TCM-d, (b) MeOH@TCM-d, (c) EtOH@TCM-d, and (d) DMF@TCM-d without Act-HKUST-1 crystals (black curves) were also measured for comparison. The ^{1}H NMR integrals were taken from the hydroxy protons (for H_2O, MeOH, and EtOH) or methyl protons (for DMF). The integral values were normalized by calibrating with the residual $CHCl_3$ in $CDCl_3$.

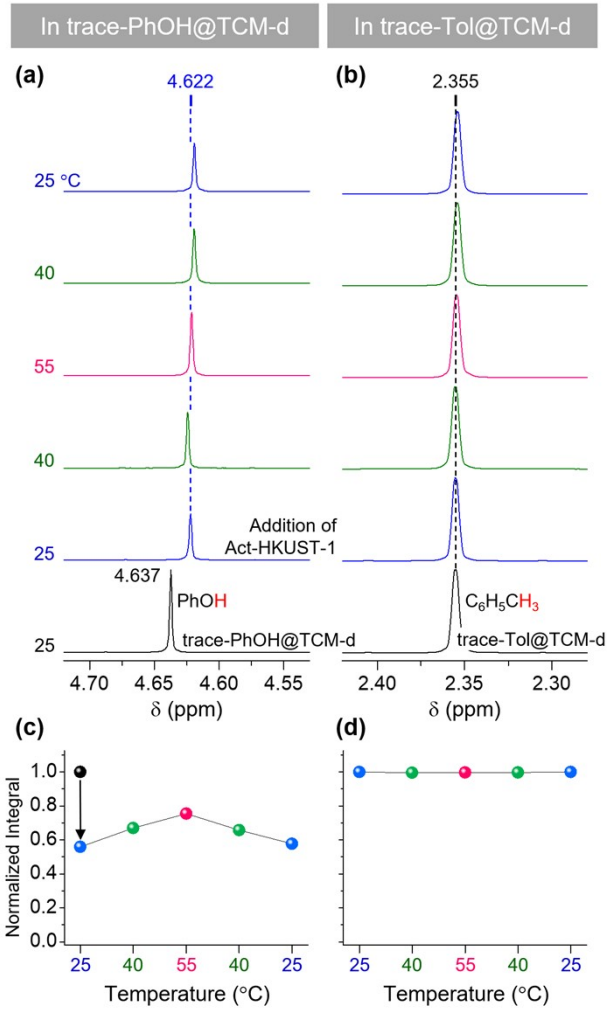

Fig. S18 (a-b) Ex-situ ^{1}H NMR spectra and (c-d) integral profiles of (a, c) PhOH in PhOH@TCM-d and (b, d) toluene in Tol@TCM-d measured at a fixed temperature of 25 °C, after taking corresponding supernatant solvents from each vial containing small Act-HKUST-1 crystals (ca. 10 μm), which was placed in a temperature-controlled oil bath at 25 °C (blue curves), 40 °C (green curves), and 55 °C (red curves), respectively. In contrast to the in situ ^{1}H NMR spectra, the chemical shifts of PhOH and Tol do not alter due to the fixed temperature (25 °C) of the NMR tube specimen. ^{1}H NMR spectra of (a, c) PhOH@TCM-d and (b, d) Tol@TCM-d without Act-HKUST-1 crystals (black curves) were also measured for comparison. The ^{1}H NMR integrals were taken from the hydroxy protons (for PhOH) or methyl protons (for toluene). The integral values were normalized by calibrating with the residual $CHCl_3$ in $CDCl_3$.

Section S10. Broad views of ex-situ ^{1}H NMR spectra recorded with small HKUST-1 crystals

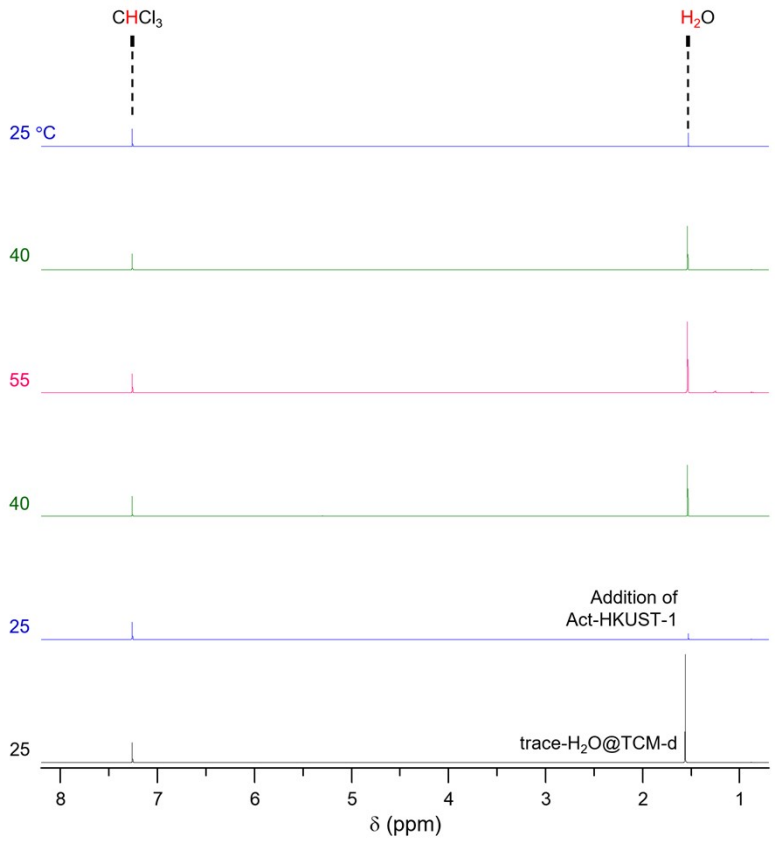

Fig. S19 Broad view of ex-situ ^{1}H NMR spectra of H_2O molecules in H_2O@TCM-d solvent measured at a fixed temperature of 25 °C after taking corresponding supernatant solvents from each vial containing small Act-HKUST-1 crystals (ca. 10 μm), which was placed in a temperature-controlled oil bath at 25 °C (blue curves), 40 °C (green curves), and 55 °C (red curves), respectively. ^{1}H NMR spectra of H_2O@TCM-d without Act-HKUST-1 crystals (black curves) were also measured for comparison.

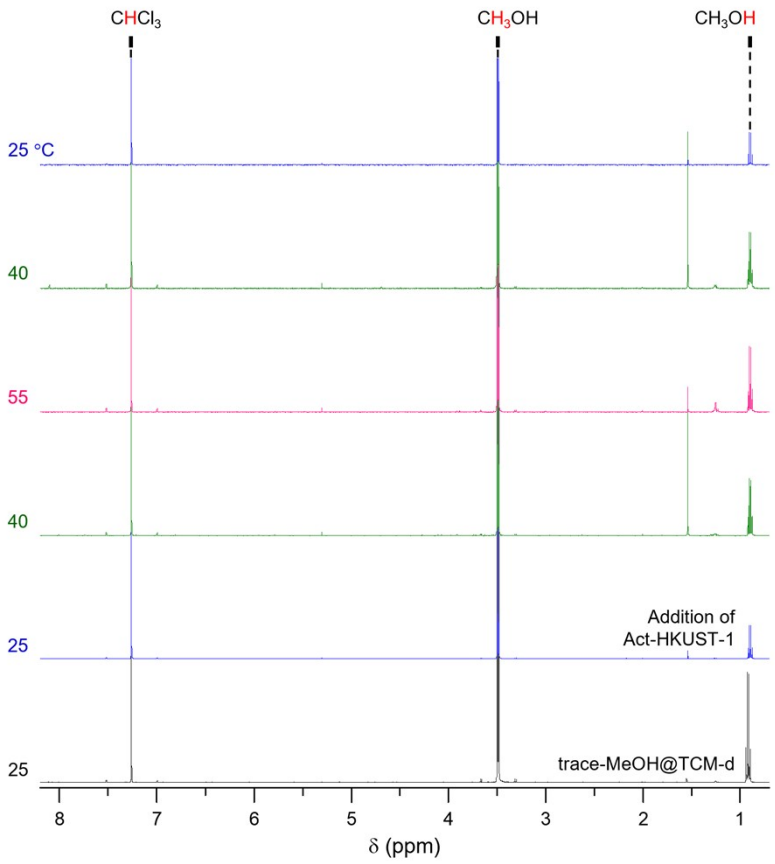

Fig. S20 Broad view of ex-situ ^{1}H NMR spectra of MeOH molecules in MeOH@TCM-d solvent measured at a fixed temperature of 25 °C after taking corresponding supernatant solvents from each vial containing small Act-HKUST-1 crystals (ca. 10 μm), which was placed in a temperature-controlled oil bath at 25 °C (blue curves), 40 °C (green curves), and 55 °C (red curves), respectively. ^{1}H NMR spectra of MeOH@TCM-d without Act-HKUST-1 crystals (black curves) were also measured for comparison.

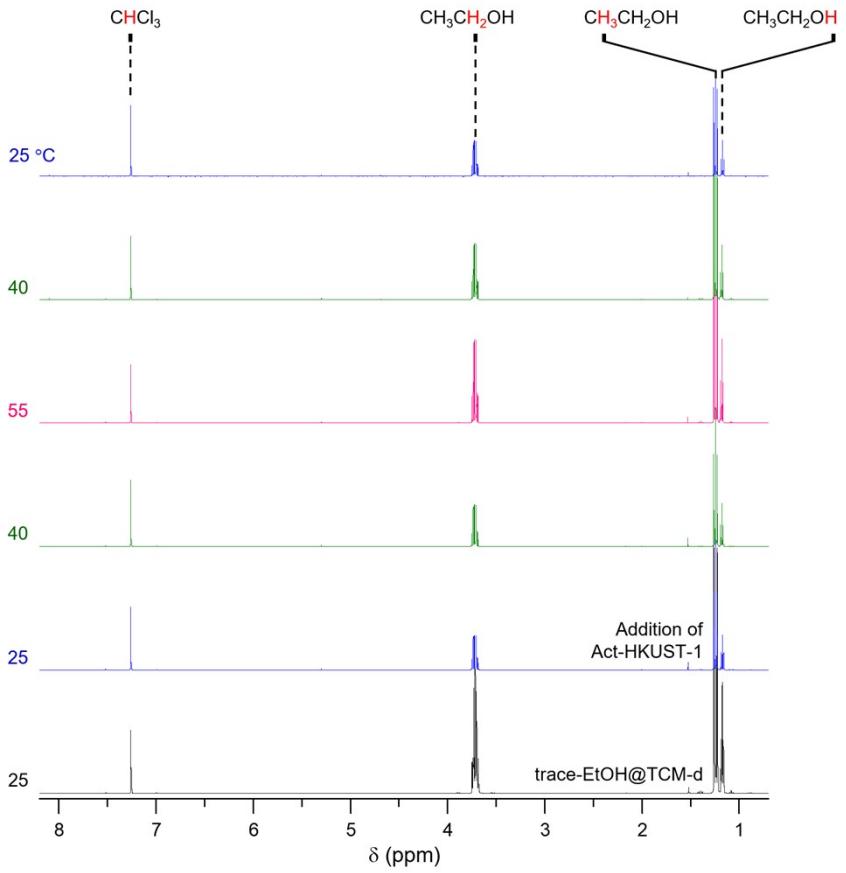

Fig. S21 Broad view of ex-situ ^{1}H NMR spectra of EtOH molecules in EtOH@TCM-d solvent measured at a fixed temperature of 25 °C after taking corresponding supernatant solvents from each vial containing small Act-HKUST-1 crystals (ca. 10 μm), which was placed in a temperature-controlled oil bath at 25 °C (blue curves), 40 °C (green curves), and 55 °C (red curves), respectively. ^{1}H NMR spectra of EtOH@TCM-d without Act-HKUST-1 crystals (black curves) were also measured for comparison.

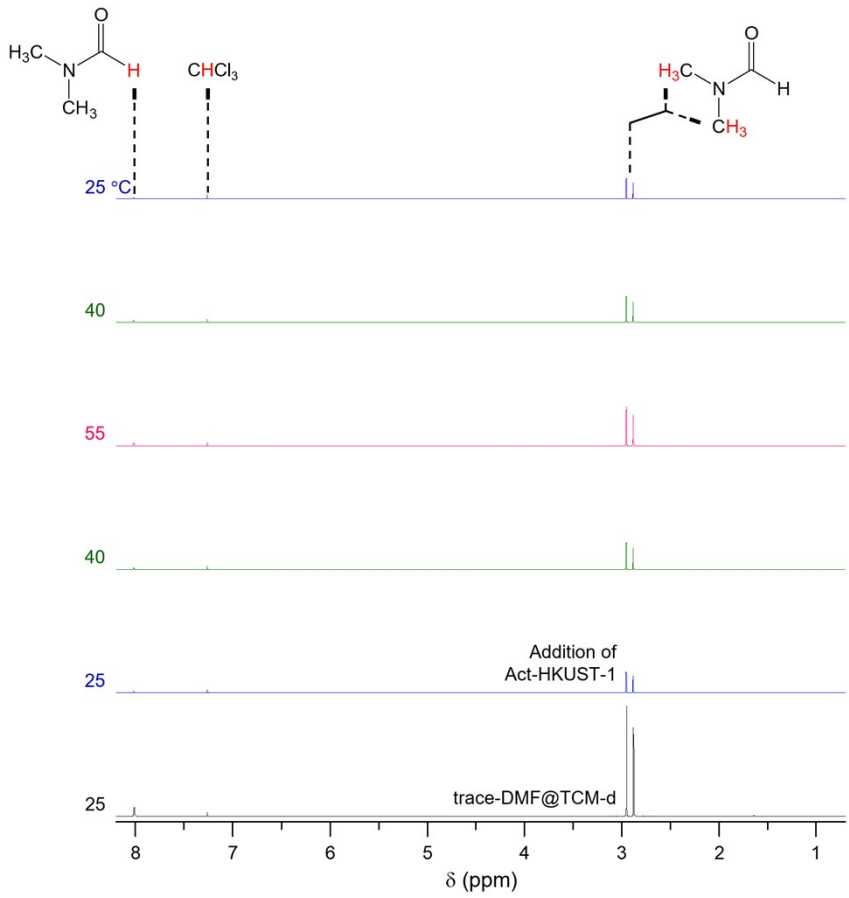

Fig. S22 Broad view of ex-situ ^{1}H NMR spectra of DMF molecules in DMF@TCM-d solvent measured at a fixed temperature of 25 °C after taking corresponding supernatant solvents from each vial containing small Act-HKUST-1 crystals (ca. 10 μm), which was placed in a temperature-controlled oil bath at 25 °C (blue curves), 40 °C (green curves), and 55 °C (red curves), respectively. ^{1}H NMR spectra of DMF@TCM-d without Act-HKUST-1 crystals (black curves) were also measured for comparison.

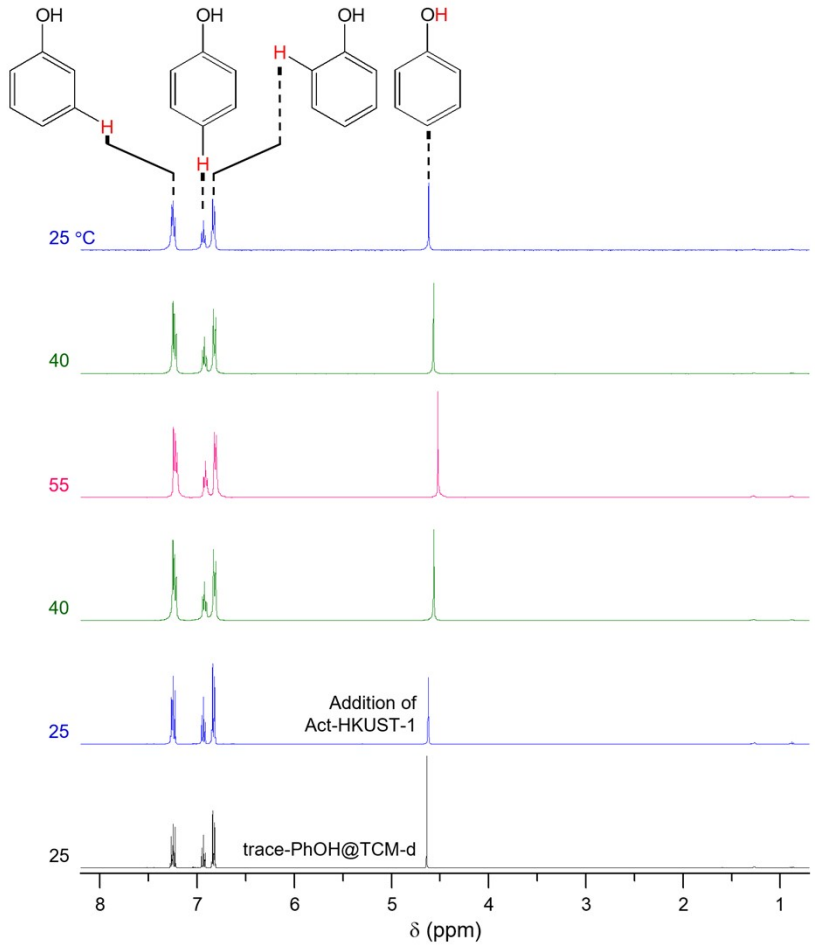

Fig. S23 Broad view of ex-situ ^{1}H NMR spectra of PhOH molecules in PhOH@TCM-d solvent measured at a fixed temperature of 25 °C after taking corresponding supernatant solvents from each vial containing small Act-HKUST-1 crystals (ca. 10 μm), which was placed in a temperature-controlled oil bath at 25 °C (blue curves), 40 °C (green curves), and 55 °C (red curves), respectively. ^{1}H NMR spectra of PhOH@TCM-d without Act-HKUST-1 crystals (black curves) were also measured for comparison.

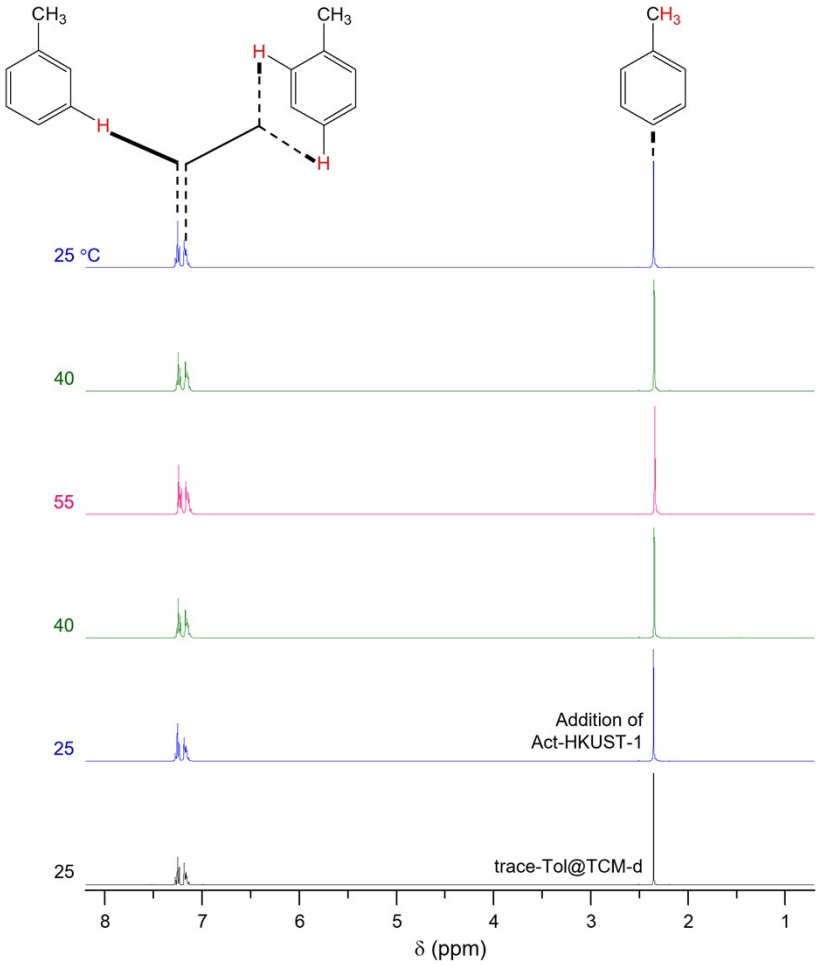

Fig. S24 Broad view of ex-situ ^{1}H NMR spectra of toluene molecules in Tol@TCM-d solvent measured at a fixed temperature of 25 °C after taking corresponding supernatant solvents from each vial containing small Act-HKUST-1 crystals (ca. 10 μm), which was placed in a temperature-controlled oil bath at 25 °C (blue curves), 40 °C (green curves), and 55 °C (red curves), respectively. ^{1}H NMR spectra of Tol@TCM-d without Act-HKUST-1 crystals (black curves) were also measured for comparison.

Section S11. Phase and chemical purities of the samples prepared for Raman studies

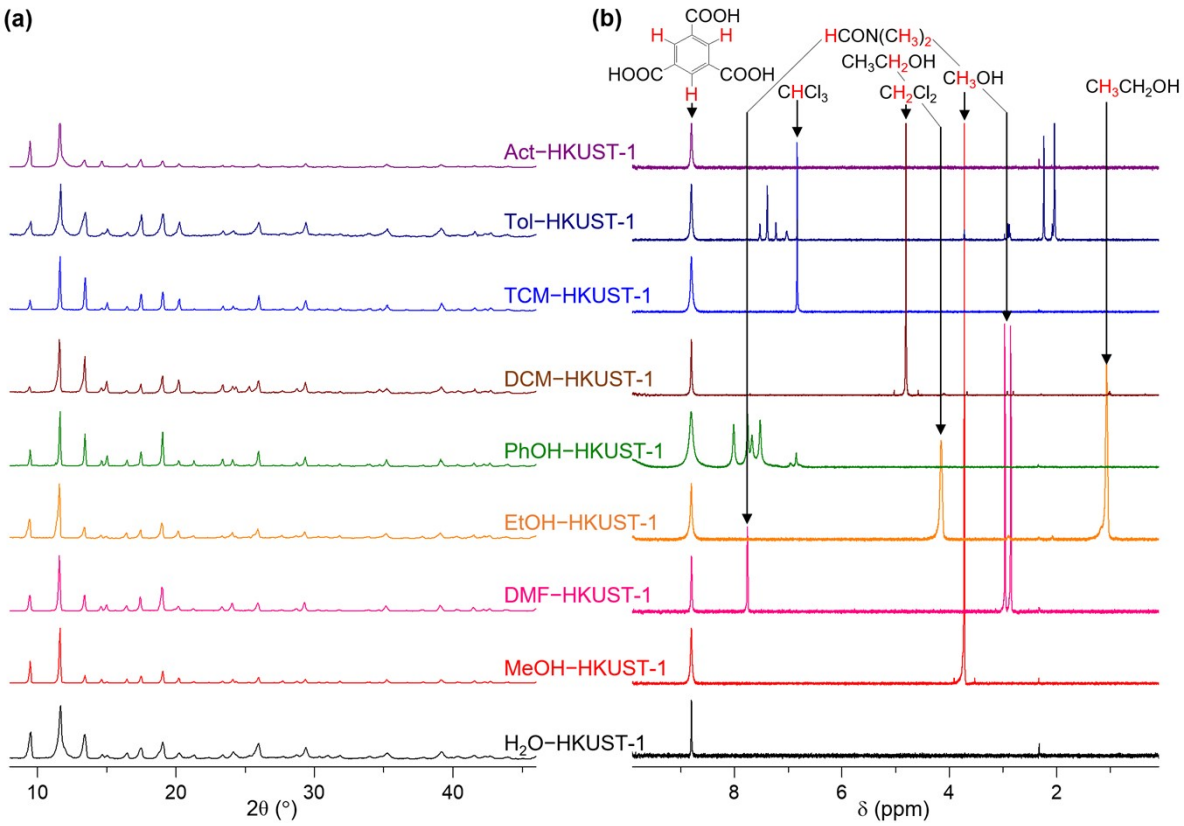

Fig. S25 (a) PXRD patterns and (b) ^{1}H NMR spectra of H_2O-, MeOH-, DMF-, EtOH-, PhOH-, DCM-, TCM-, and Tol-HKUST-1 samples, which were examined for Raman spectroscopic analysis. Act-HKUST-1 was also examined for comparison. ^{1}H NMR spectra were recorded after the samples were entirely dissolved in concentrated deuterated sulfuric acid, D_2SO_4.

Section S12. Single crystal X-ray crystallography of water-included TCM-HKUST-1 and water-excluded TCM-HKUST-1 crystals

The structures reported in this manuscript were solved by following the general method for all MOF structures whose crystals:

- are prepared in single crystal-to-single crystal multi-step sequences involving numerous solvents washing steps and activation of the crystals;
- have significant X-ray diffuse scattering from guest solvent molecules in the pore network.

These factors all create challenges for the structure determination and are shown by a handful of level A/B alerts registered by standard checking software.

Water-included TCM-HKUST-1 crystal

Suitable single crystals of HKUST-1 were synthesized following the procedure reported previously.[1] For the water-included TCM-HKUST-1 crystal, the sample was activated under vacuum at 90 °C for 12 hours. Subsequently, the crystal was exposed to water-included TCM and mounted in Parabar 10312 (Hampton Research Inc.) on a MiteGen micro-loop, and X-ray diffraction was collected at 150(2) K on a D8 Venture (Bruker) equipped with a Mo X-ray tube (Kα1 = 0.7107 Å, 50 kV, and 30 mA). The data set was corrected by eliminating X-ray absorption, and the structure was solved by direct methods using SHELXS[5] and refined by full-matrix least-squares on F^2 by SHELXL.[6] All non-hydrogen atoms were refined anisotropically, and all hydrogen atoms were placed in geometrically idealized positions and constrained to ride on their parent atom with C—H = 0.93 Å with U_{iso}(H) values of 1.2 U_{eq} of the parent atom. The hydrogen atoms of the coordinated water molecule were assigned based on a different Fourier map and were refined with distance restraints of 0.922(7)Å (using DFIX and DANG commands), and U_{iso}(H) values of 1.5 U_{eq} of the oxygen atom. The pore-filling solvent was highly disordered in the crystal system; all the attempts to locate and refine the solvent peaks were unsuccessful. Thus, the final refinement was performed with the structural factors modified based on the disordered structural solvent electron densities obtained from the SQUEEZE routine of PLATON.

Water-excluded TCM-HKUST-1 crystal

For the water-excluded TCM-HKUST-1 crystal, a crystal was mounted in a capillary tube with a diameter of 0.8 mm, which contained a smear of Parabar 10312 (Hampton Research Inc.) inside to restrain the movement of the crystal (Fig. S25). The crystal was activated to remove the pore-filling solvent at 90 °C for 16 hours and stored inside a moisture-free glove box. Further, HKUST-1 crystal was exposed to water-excluded TCM vapour (the absence of water was corroborated via ^{1}H NMR prior to use) for 12 hours (Fig. S26). Finally, the capillary was sealed with epoxy glue to guarantee the isolation of the crystal from the ambient air. The X-ray diffraction of the crystal was collected at 150(2) K on a D8 Venture (Bruker) equipped with a Mo X-ray tube (Kα1 = 0.7107 Å, 50 kV, and 30 mA). The data set was corrected by eliminating X-ray absorption, and the crystal structure was solved by direct methods using SHELXS[5] and refined by full-matrix least-squares on F^2 by SHELXL.[6] All non-hydrogen atoms were refined anisotropically, and all hydrogen atoms were placed in geometrically idealized positions and constrained to ride on their parent atom with C—H = 0.93 Å with U_{iso}(H) values of 1.2 U_{eq} of the parent atom. The TCM coordinated to the Cu(II) paddlewheel complexes had a relatively low occupancy (0.5) due to the disorder of the molecule. Moreover, because of the high symmetry of the structure, the TCM molecule could not be adequately modelled. The structural solvents were highly disordered in the crystal system, and the attempts to locate and refine the solvent peaks were unsuccessful. Thus, the final refinement was performed with the structural factors modified based on the disordered structural solvent electron densities obtained from the SQUEEZE routine of PLATON.

The complete data set for the determination of the crystal structures has been deposited in the Cambridge Crystallographic Data Centre with the CCDC reference numbers of 2184392 and 2184185. The copies of this information may be obtained free of charge from the director, CCDC, 12 Union Street, Cambridge CB2 1EZ, U.K. (fax, +44-1223-336-033; email, deposit@ccdc.cam.ac.uk). The table below provides the crystal data and structure refinement details for water-excluded TCM-HKUST-1 and water-included TCM-HKUST-1.

Table S1. Crystal data and structure refinement of water-excluded TCM-HKUST-1 and water-included TCM-HKUST-1 crystals.

Identification code	**Water-excluded TCM-HKUST-1**	**Water-included TCM-HKUST-1**
Empirical formula	C_{37} H_{13} Cl_3 Cu_6 O_{24}	$C_{36}H_{24}Cu_6O_{30}$
Formula weight	1316.05	1317.79
Temperature/K	150 (2)	150 (2)
Crystal system	cubic	cubic
Space group	Fm-3m	Fm-3m
a/Å	26.3444(12)	26.2909(13)
b/Å	26.3444(12)	26.2909(13)
c/Å	26.3444(12)	26.2909(13)
α/°	90	90
β/°	90	90
γ/°	90	90
Volume/Å^3	18284(2)	18173(3)
Z	8	8
ρ_{calcg}/cm^3	0.956	0.963
μ/mm^{-1}	1.501	1.430
F(000)	5160	5232.0
Crystal size/mm^3	0.21 × 0.135 × 0.118	0.125 × 0.121 × 0.105
Θ range for data collection/°	2.187 to 27.996	2.191 to 27.244
Index ranges	-34≤h≤34, -34≤k≤34, -34≤l≤34	-33≤h≤33, -33≤k≤33, -33≤l≤33
Reflections collected	106390	171923
Independent reflections	1164 [R_{int} = 0.3120]	1065 [R_{int} = 0.2517]
Data/restraints/parameters	1164/0/36	1065/3/38
Goodness-of-fit on F^2	1.103	1.111
Final R indexes [I>=2σ (I)]	R1 = 0.0561, wR_2 = 0.1633	R1 = 0.0503, wR_2 = 0.1318
Final R indexes [all data]	R1 = 0.0676, wR_2 = 0.1839	R1 = 0.0650, wR_2 = 0.1425
Largest diff. peak/hole / e Å^{-3}	0.70/-1.22	0.519/-1.681
CCDC Number	2184392	2184185

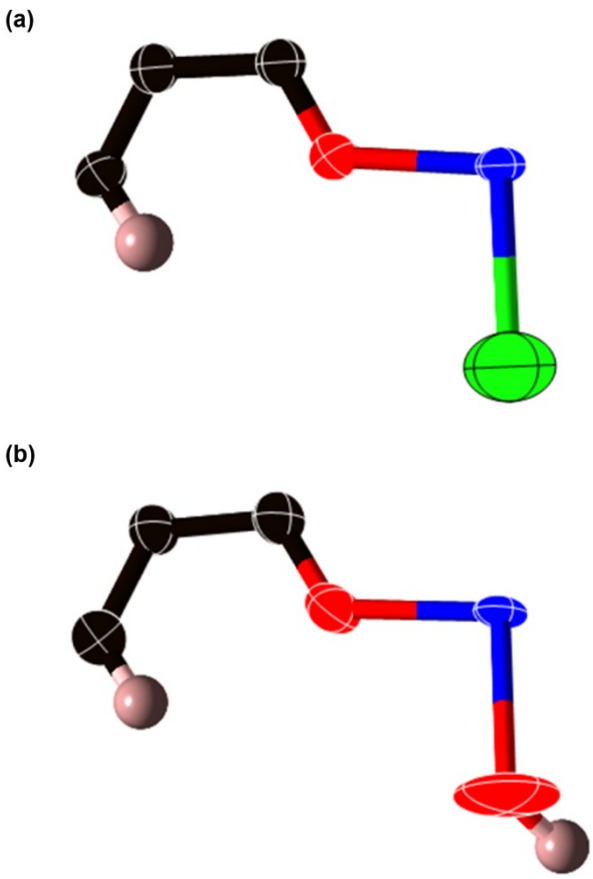

Fig. S26 The asymmetric unit of (a) Water-excluded TCM-HKUST-1 and (b) Water-included TCM-HKUST-1, with all non-hydrogen atoms represented by ellipsoids at the 50% probability level (C, black; H, white; O, red; Cu, blue; Cl, green).

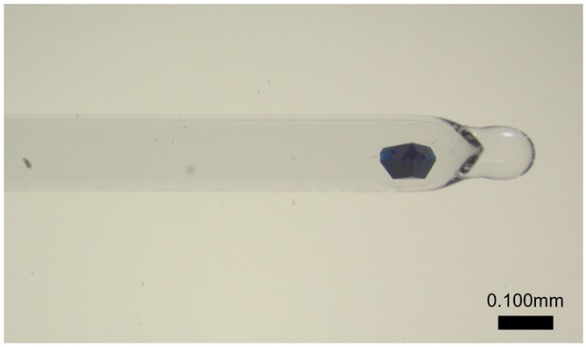

Fig. S27 A capillary tube containing an activated HKUST-1 single crystal prepared for the X-Ray crystallography.

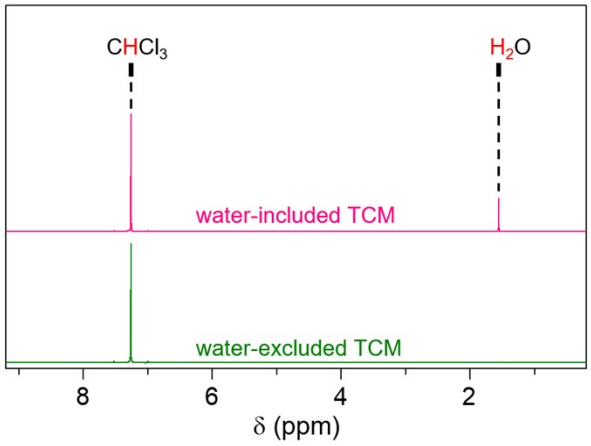

Fig. S28 ^{1}H NMR spectra of water-excluded and -included TCM

Section S13. Conversion profiles of the catalytic hydrogenation of acetophenone performed in various solvents

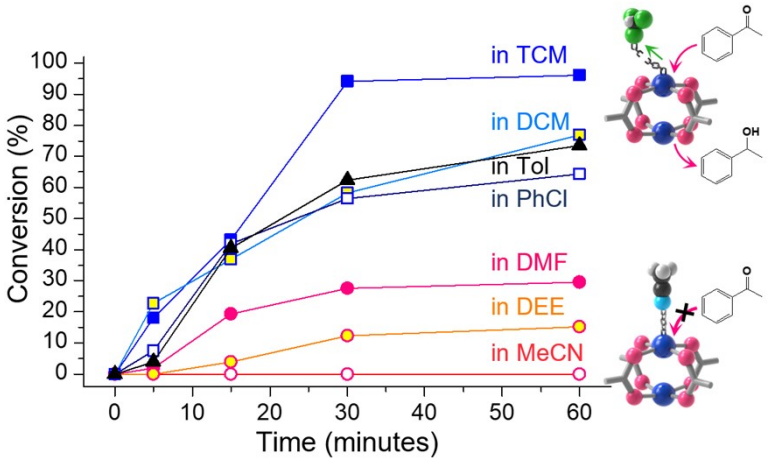

Fig. S29 Conversion profiles of the catalytic hydrogenation reaction of acetophenone performed in MeCN (orange-red curve with open circles), DEE (orange curve with yellow open circles), DMF (pink curve with closed circles), PhCl (dark cyan curve with open blue squares), Tol (black curve with closed triangles), DCM (sky blue curve with open yellow squares), and TCM (blue curve with closed squares).

Section S14. ^{1}H NMR spectra for the catalytic hydrogenations of acetophenone with Act-HKUST-1

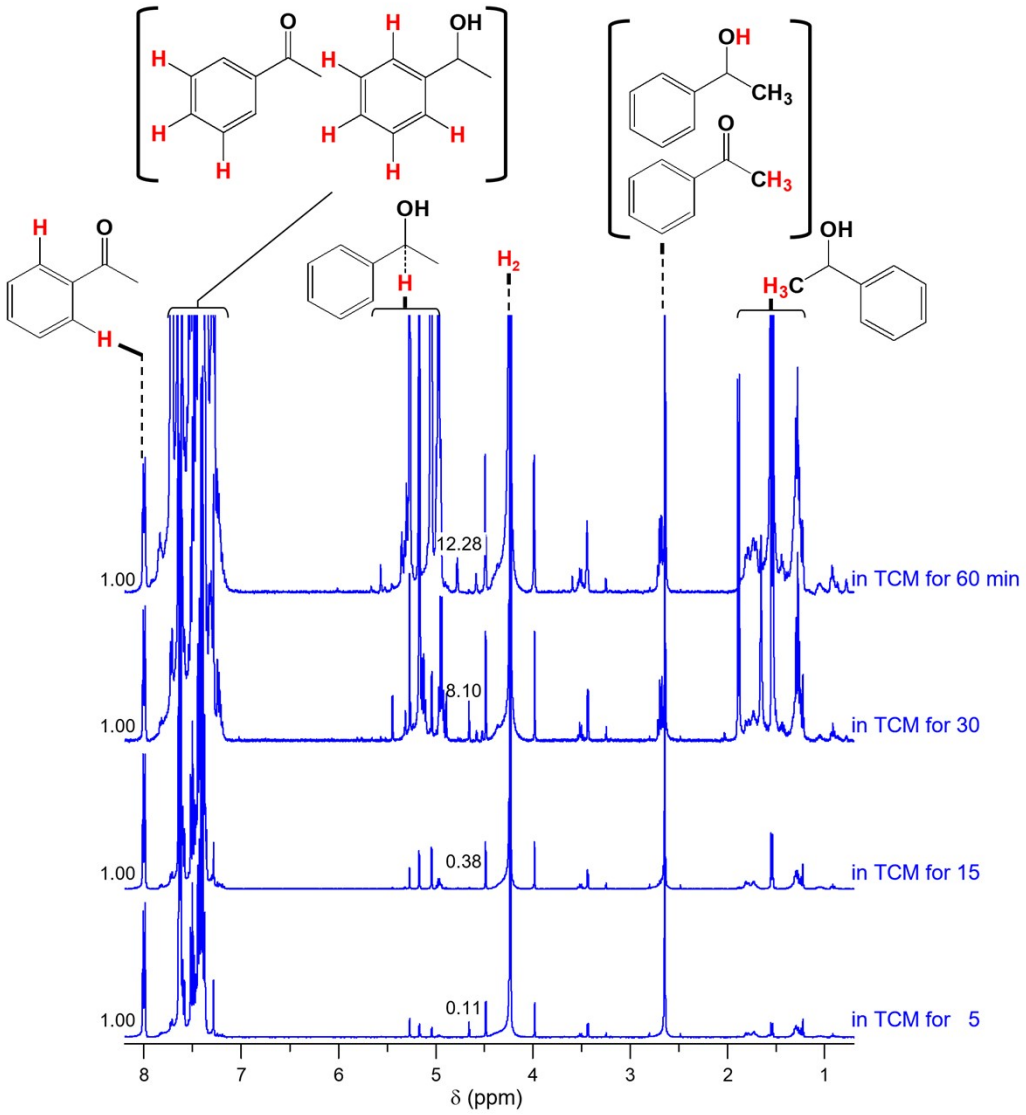

Fig. S30 ^{1}H NMR spectra of a TCM solution, where the catalytic hydrogenation reaction of acetophenone with Act-HKUST-1 crystals was undergone. Each solution was taken after the reaction was carried out for 5, 15, 30, and 60 minutes. The conversion efficiencies of acetophenone to 1-phenylethanol in TCM solvent were calculated by comparing the integrals of benzylic proton of 1-phenylethanol appearing at around 4.8-5.6 ppm versus the phenyl ortho-protons of acetophenone appearing at around 8.00 ppm.

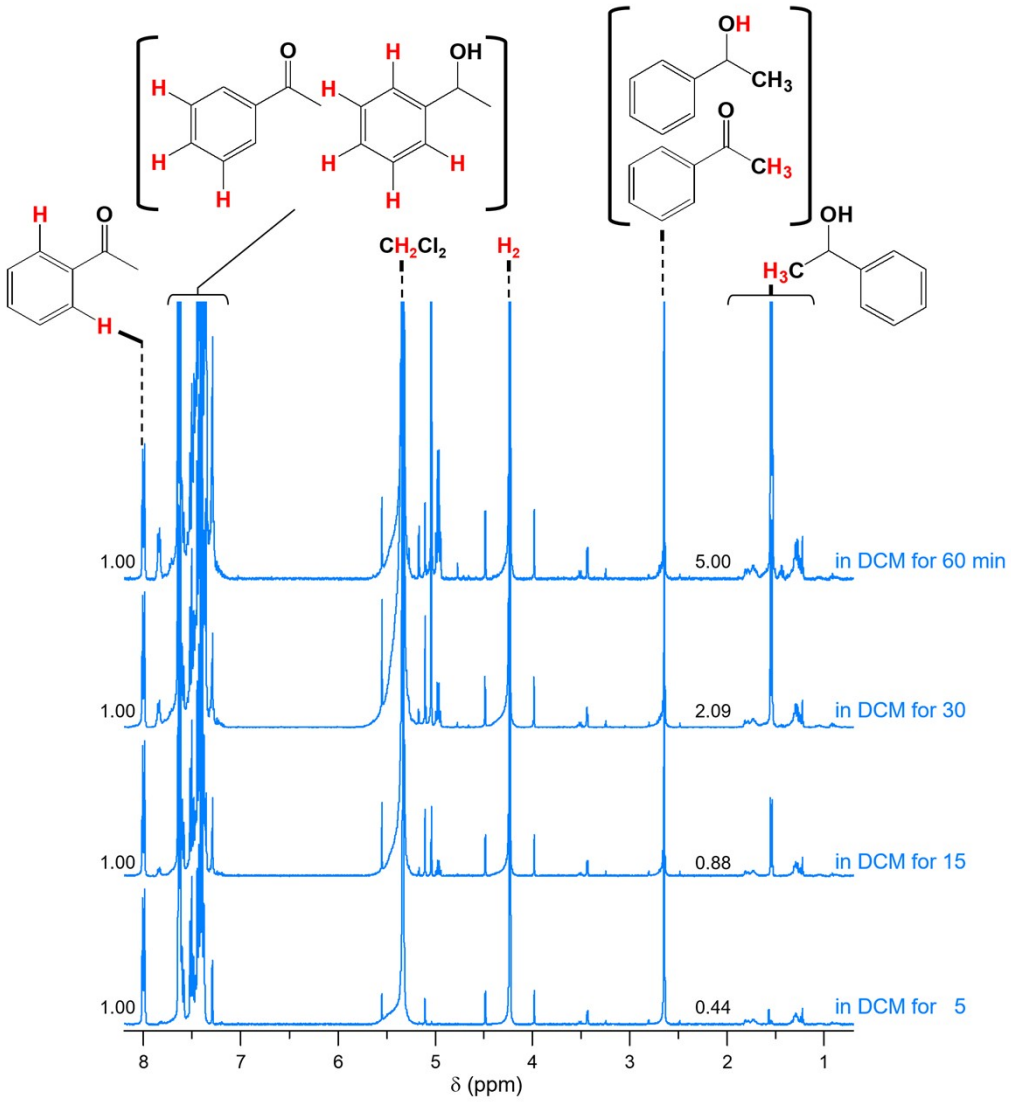

Fig. S31 ^{1}H NMR spectra of a DCM solution, where the catalytic hydrogenation reaction of acetophenone with Act-HKUST-1 crystals was undergone. Each solution was taken after the reaction was carried out for 5, 15, 30, and 60 minutes. The conversion efficiencies of acetophenone to 1-phenylethanol in DCM solvent were calculated by comparing the integrals of methyl protons of 1-phenylethanol appearing at 1.55 ppm versus the phenyl ortho-protons of acetophenone appearing at around 8.00 ppm.

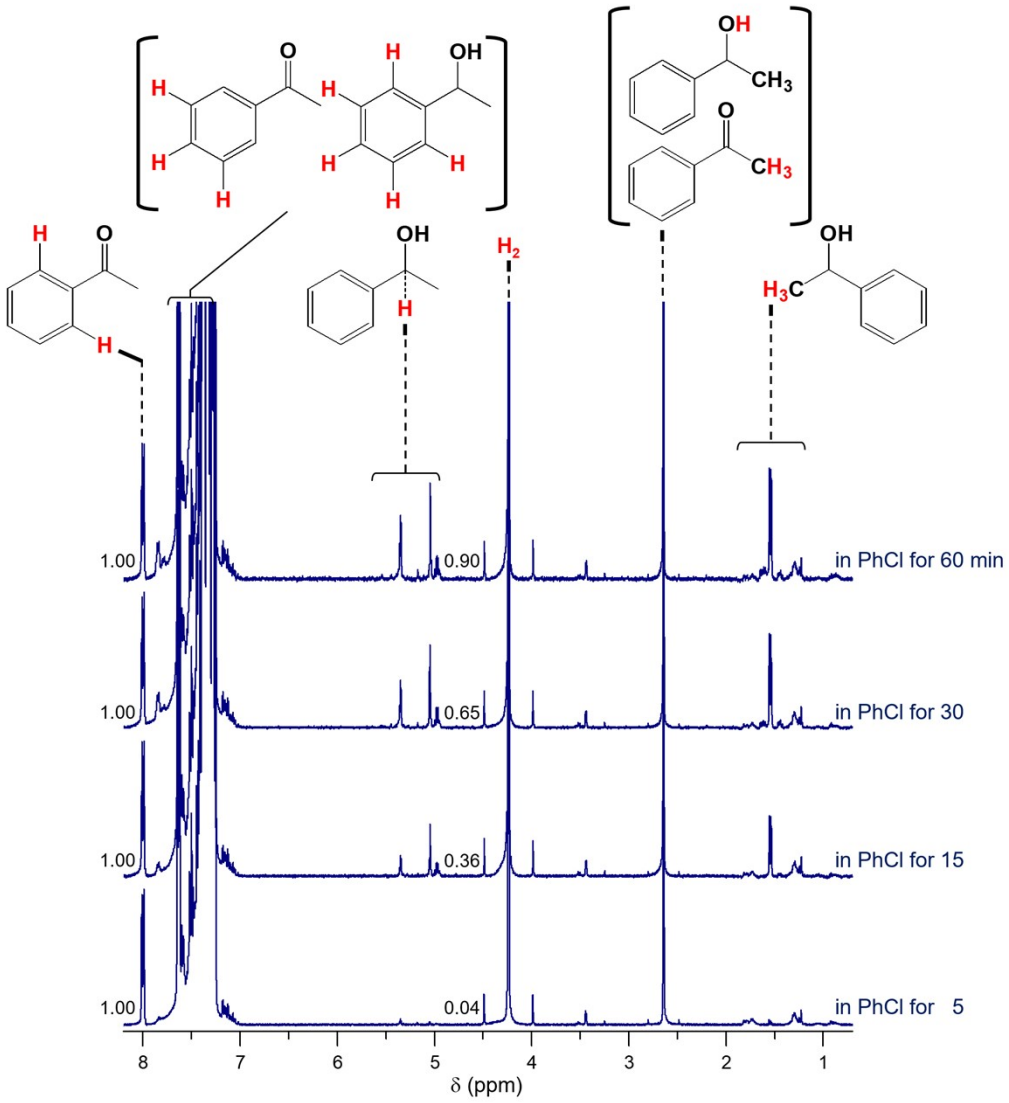

Fig. S32 ^{1}H NMR spectra of a PhCl solution, where the catalytic hydrogenation reaction of acetophenone with Act-HKUST-1 crystals was undergone. Each solution was taken after the reaction was carried out for 5, 15, 30, and 60 minutes. The conversion efficiencies of acetophenone to 1-phenylethanol in PhCl were calculated by comparing the integrals of benzylic proton of 1-phenylethanol appearing at around 4.8-5.6 ppm versus the phenyl ortho-protons of acetophenone appearing at around 8.00 ppm.

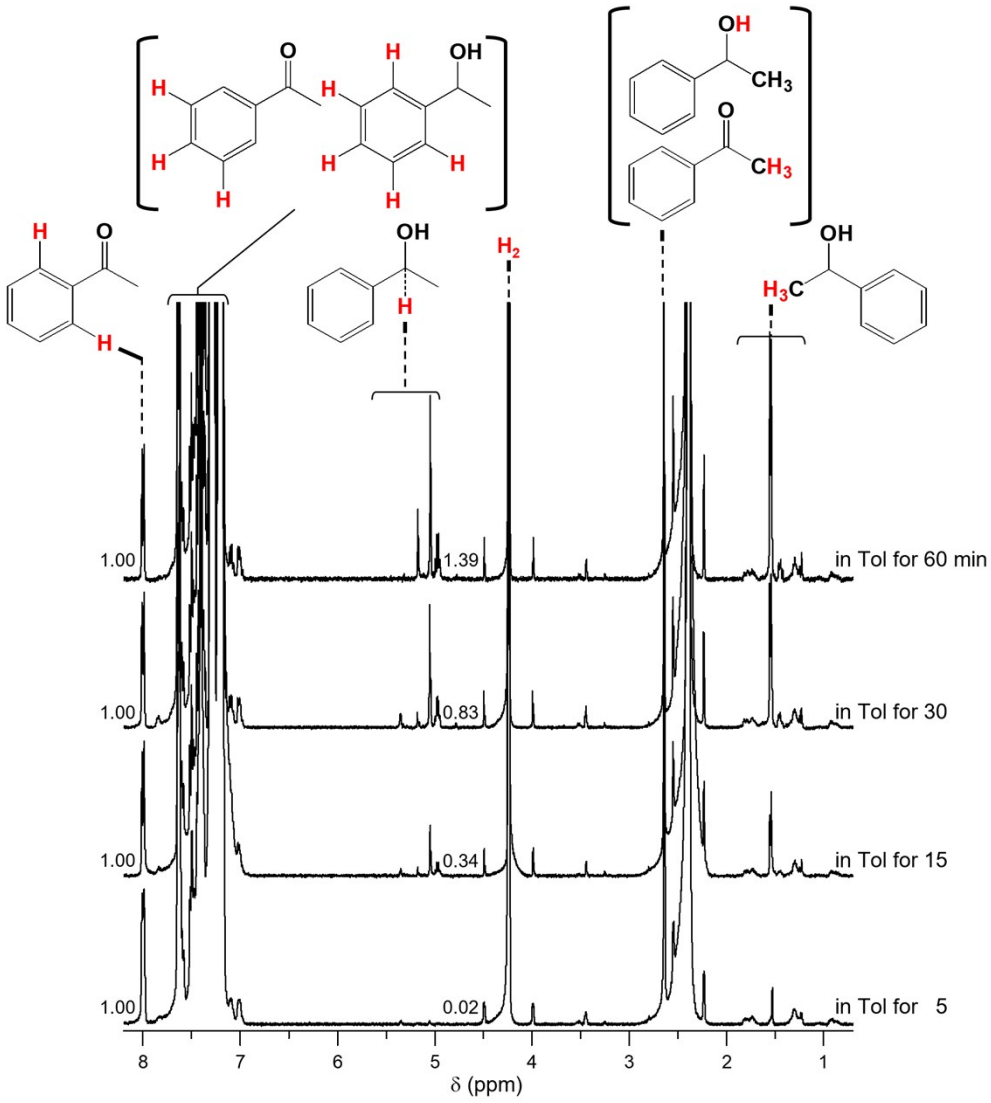

Fig. S33 ^{1}H NMR spectra of a toluene solution, where the catalytic hydrogenation reaction of acetophenone with Act-HKUST-1 crystals was undergone. Each solution was taken after the reaction was carried out for 5, 15, 30, and 60 minutes. The conversion efficiencies of acetophenone to 1-phenylethanol in toluene were calculated by comparing the integrals of benzylic proton of 1-phenylethanol appearing at around 4.8-5.6 ppm versus the phenyl ortho-protons of acetophenone appearing at around 8.00 ppm.

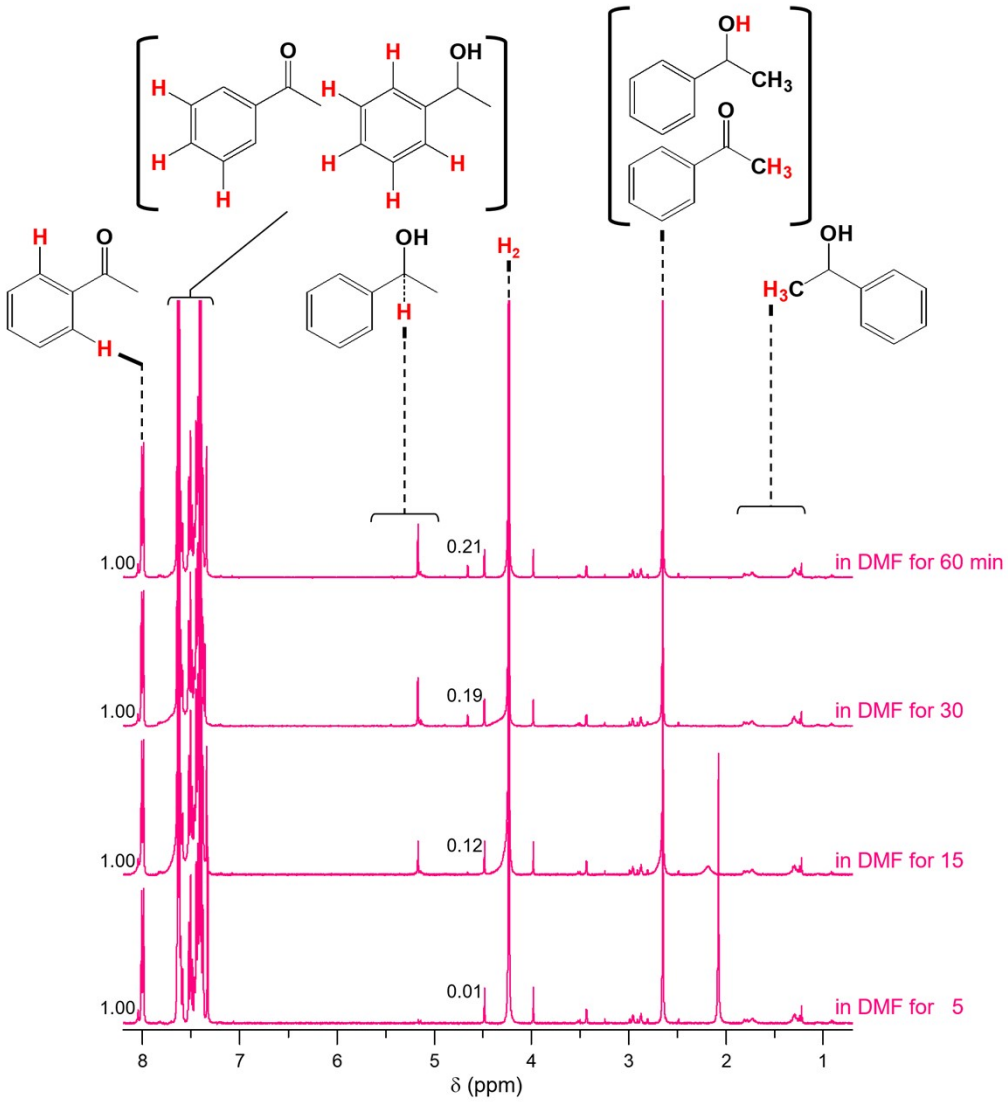

Fig. S34 ^{1}H NMR spectra of a DMF solution, where the catalytic hydrogenation reaction of acetophenone with Act-HKUST-1 crystals was undergone. Each solution was taken after the reaction was carried out for 5, 15, 30, and 60 minutes. The conversion efficiencies of acetophenone to 1-phenylethanol in DMF were calculated by comparing the integrals of benzylic proton of 1-phenylethanol appearing at around 4.8-5.6 ppm versus the phenyl ortho-protons of acetophenone appearing at around 8.00 ppm.

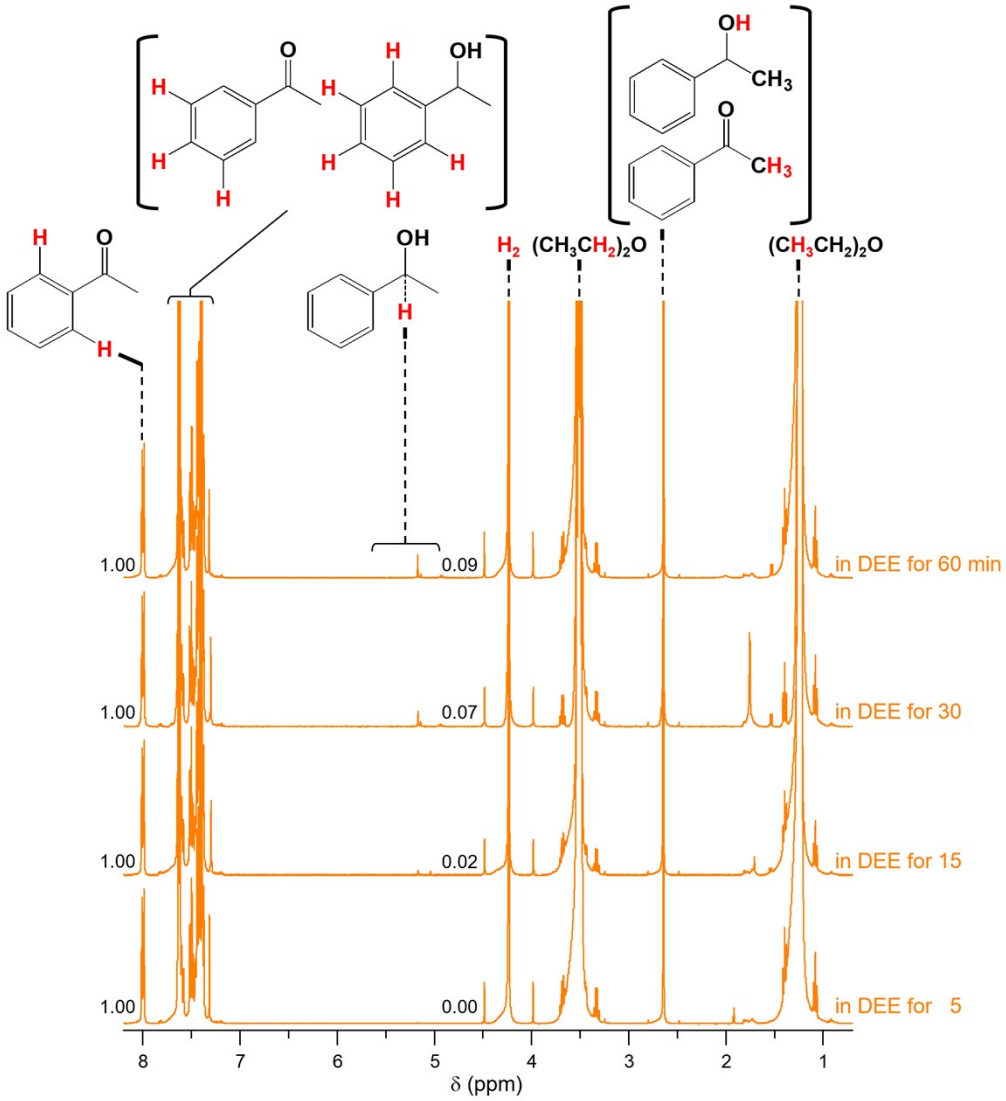

Fig. S35 ^{1}H NMR spectra of DEE solution, where the catalytic hydrogenation reaction of acetophenone with Act-HKUST-1 crystals was undergone. Each solution was taken after the reaction was carried out for 5, 15, 30, and 60 minutes. The conversion efficiencies of acetophenone to 1-phenylethanol in DEE were calculated by comparing the integrals of benzylic proton of 1-phenylethanol appearing at around 4.8-5.6 ppm versus the phenyl ortho-protons of acetophenone appearing at around 8.00 ppm.

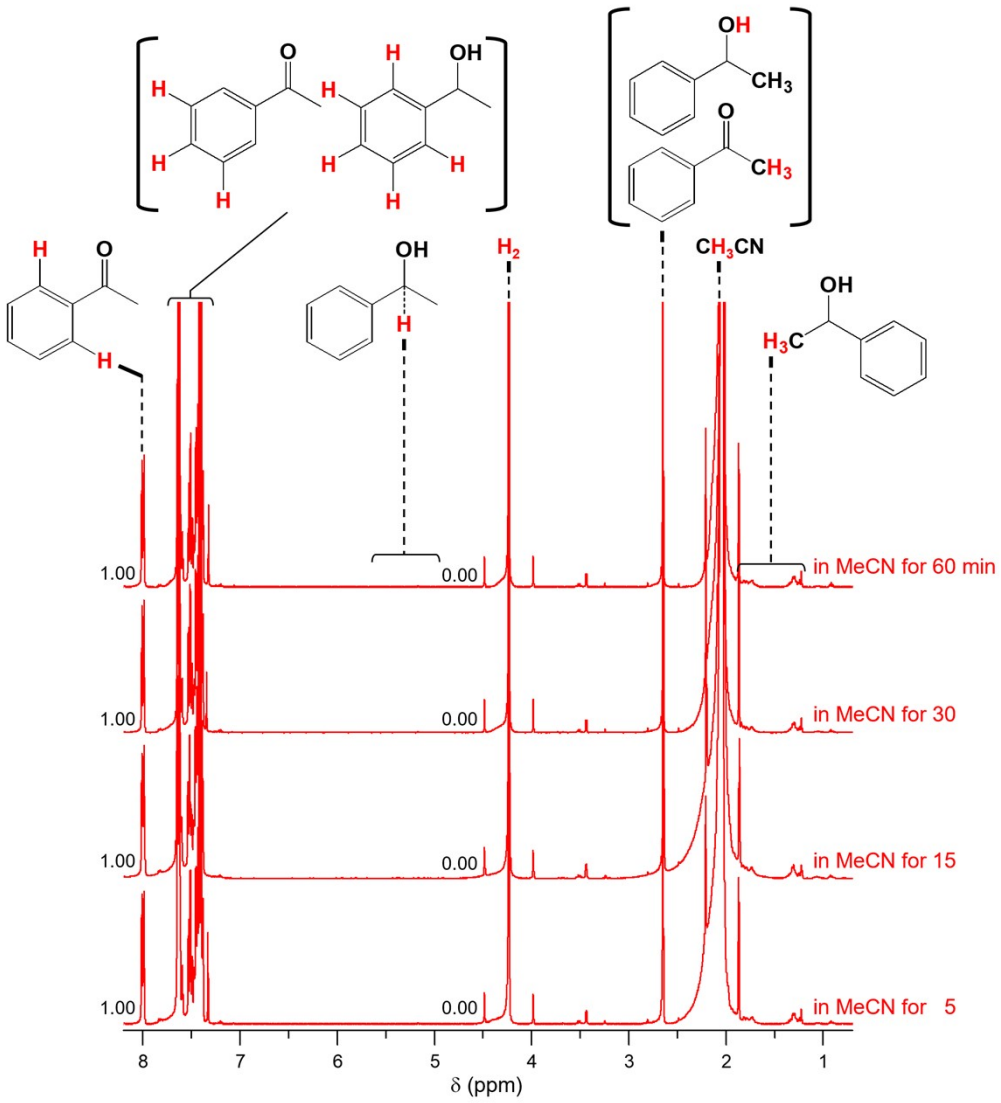

Fig. S36 ^{1}H NMR spectra of an MeCN solution, where the catalytic hydrogenation reaction of acetophenone with Act-HKUST-1 crystals was undergone. Each solution was taken after the reaction was carried out for 5, 15, 30, and 60 minutes. The conversion efficiencies of acetophenone to 1-phenylethanol in MeCN were calculated by comparing the integrals of benzylic proton of 1-phenylethanol appearing at around 4.8-5.6 ppm versus the phenyl ortho-protons of acetophenone appearing at around 8.00 ppm.

Section S15. ^{1}H NMR spectra for the catalytic hydrogenations of acetone with Act-HKUST-1

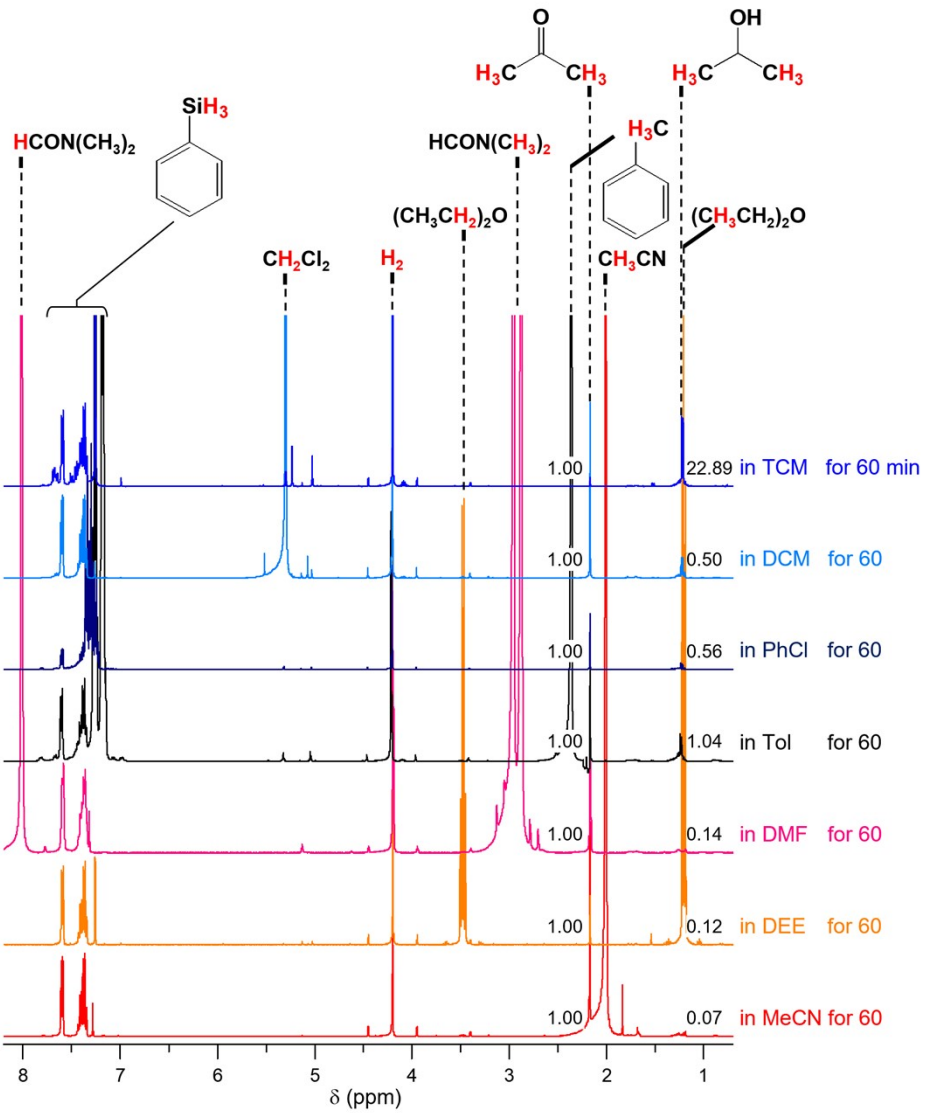

Fig. S37 ^{1}H NMR spectra of the supernatant solutions of MeCN, DEE, DMF, Tol, PhCl, DCM, and TCM, where the catalytic hydrogenation reactions of acetone with Act-HKUST-1 crystals were undergone. Each solution was taken after the reaction was carried out for 60 minutes. The conversion efficiencies of acetone to isopropanol were calculated by comparing the integrals of methyl protons of isopropanol appearing at around 1.22 ppm versus the methyl protons of acetone appearing at around 2.17 ppm.

References

1 H. K. Kim, W. S. Yun, M. B. Kim, J. Y. Kim, Y. S. Bae, J. Lee and N. C. Jeong, *J. Am. Chem. Soc.*, 2015, **137**, 10009-10015.
2 D. Song, J. Bae, H. Ji, M. B. Kim, Y. S. Bae, K. S. Park, D. Moon and N. C. Jeong, *J. Am. Chem. Soc.*, 2019, **141**, 7853-7864.
3 J. Bae, J. S. Choi, S. Hwang, W. S. Yun, D. Song, J. Lee and N. C. Jeong, *ACS Appl. Mater. Interfaces*, 2017, **9**, 24743-24752.
4 H. I. Song, J. Bae, E. J. Lee, K. O. Kirlikovali, O. K. Farha and N. C. Jeong, *J. Phys. Chem. C*, 2020, **124**, 13187-13195.
5 G. Sheldrick, *Acta Crystallogr. A*, 1990, **46**, 467-473.
6 G. M. Sheldrick, *Acta Crystallogr A*, 2008, **64**, 112-122.